Title

Functional host-specific adaptation of the intestinal microbiome in hominids

Authors

Rühlemann MC[1,2,†], Bang C[1], Gogarten JF[3,4,5,6], Hermes BM[7,8], Groussin M[1], Waschina S[9], Poyet M[8], Ulrich M[4,5], Akoua-Koffi C[10], Deschner T[11], Muyembe-Tamfum JJ[12], Robbins MM[13], Surbeck M[14,15], Wittig RM[16,17], Zuberbühler K[18,19], Baines JF[7,8], Leendertz FH[4,5], Franke A[1,†]

Affiliations

1 Institute of Clinical Molecular Biology, Kiel University, Kiel, Germany
2 Institute for Medical Microbiology and Hospital Epidemiology, Hannover Medical School Hannover, Germany
3 Applied Zoology and Nature Conservation, University of Greifswald, Greifswald, Germany
4 Helmholtz Institute for One Health, Helmholtz-Centre for Infection Research (HZI), Greifswald, Germany
5 Epidemiology of Highly Pathogenic Microorganisms, Robert Koch Institute, Berlin, Germany
6 Viral Evolution, Robert Koch Institute, Berlin, Germany
7 Evolutionary Genomics, Max Planck Institute for Evolutionary Biology, Plön, Germany
8 Institute of Experimental Medicine, Kiel University, Kiel, Germany
9 Nutriinformatics Research Group, Institute for Human Nutrition and Food Science, Kiel University, Kiel, Germany
10 Training and Research Unit for in Medical Sciences, Alassane Ouattara University / University Teaching Hospital of Bouaké, Bouaké, Côte d'Ivoire
11 Comparative BioCognition, Institute of Cognitive Science, University of Osnabrück, Osnabrück, Germany
12 National Institute for Biomedical Research, National Laboratory of Public Health, Kinshasa, Democratic Republic of the Congo
13 Department of Primate Behavior and Evolution, Max Planck Institute for Evolutionary Anthropology, Leipzig, Germany
14 Department of Human Evolutionary Biology, Harvard University, Cambridge, Massachusetts, United States of America
15 Max Planck Institute for Evolutionary Anthropology, Leipzig, Germany
16 Institute of Cognitive Sciences, CNRS UMR5229 University Lyon 1, Bron Cedex, France
17 Taï Chimpanzee Project, CSRS, Abidjan, Côte d'Ivoire
18 Institute of Biology, University of Neuchatel, Neuchatel, Switzerland
19 School of Psychology & Neuroscience, University of St Andrews, St Andrews, Scotland (UK)

† To whom correspondence may be addressed. Email: m.ruehlemann@ikmb.uni-kiel.de or a.franke@mucosa.com

Summary

Fine-scale knowledge of the changes in composition and function of the human gut microbiome compared that of our closest relatives is critical for understanding the evolutionary processes underlying its developmental trajectory. To infer taxonomic and functional changes in the gut microbiome across hominids at different timescales, we performed high-resolution metagenomic-based analyses of the fecal microbiome from over two hundred samples including diverse human populations, as well as wild-living chimpanzees, bonobos, and gorillas. We find human-associated taxa depleted within non-human apes and patterns of host-specific gut microbiota, suggesting the widespread acquisition of novel microbial clades along the evolutionary divergence of hosts. In contrast, we reveal multiple lines of evidence for a pervasive loss of diversity in humans populations in correlation with a high Human Development Index, including evolutionarily conserved clades. Similarly, patterns of co-phylogeny are found to be disrupted in humans. Together with identifying individual microbial taxa and functional adaptations that correlate to host phylogeny, these findings offer new and exciting insights into specific candidates playing a role in the diverging trajectories of the gut microbiome of hominids, demonstrating that repeated horizontal gene transfer and gene loss, as well as the adaptation to transient microaerobic conditions appear to have played a role in the evolution of the human gut microbiome.

Introduction

Human gut microbiome research has demonstrated that numerous factors, including diet, environment, and lifestyle influence the structure of the human gut microbiota, which in turn have profound impacts on human health and disease (Johnson et al., 2019; Lloyd-Price et al., 2019; Vangay et al., 2018). To date, the majority of these studies were conducted on sample collections from high-income countries, however growing efforts to include humans from diverse global populations are underway, thereby providing an additional angle to investigate and evaluate shared and specific microbiome properties across human populations (McCall et al., 2020; Schaan et al., 2021; E. D. Sonnenburg and Sonnenburg, 2019; Vangay et al., 2018). These efforts provided an opportunity to discover signatures of host geography and lifestyle that go beyond conventional differences in diversity parameters in the gut community. For

instance, they revealed elevated rates of horizontal gene transfer (HGT) that correlate with the Human Development Index (HDI, a statistical composite index of indicators encompassing life expectancy, education, and income; (UNDP (United Nations Development Programme), 2022)) of a population, suggesting that gut microbiota constantly acquire new functions in conjunction with host lifestyle changes (Groussin et al., 2021). However, the mechanisms that link changes in gut microbial structure with host behavior and ecology remain largely unexplored.

Additional critical insight into understanding patterns of diversity and composition among human gut communities can be obtained from comparative surveys of the hominid gut microbiota. Humans, chimpanzees, bonobos, and gorillas show increasingly divergent gut microbiota, with more distantly related species exhibiting more divergent community composition (phylosymbiosis; (Brooks et al., 2016)). At the same time, the phylogeny of some of their individual microbial lineages parallels their own phylogeny (codivergence; (Groussin et al., 2020; Suzuki et al., 2022)). Both patterns of phylosymbiosis and codivergence are suggestive of long-term effects of hominid evolution on their communities of symbionts (Groussin et al., 2017; Moeller et al., 2016; Ochman et al., 2010). Notably, results from comparative marker-gene analyses suggest co-diversifying members of the hominid gut microbial communities (both prokaryotic and phage) are lost and replaced with human lineages when animals leave their natural environments and are moved into captivity (Gogarten et al., 2021; Nishida and Ochman, 2021). However, poor taxonomic resolution and a lack of functional characterization precludes a deeper understanding of processes driving these changes.

Functional analyses from shotgun metagenomic data revealed a conserved phylogenetic signal across wild non-human primates (NHP), despite dietary changes over an individual's lifespan and between species, suggesting that the evolution of gut microbiota within wild NHP is partially constrained by host genetics and physiology (Amato et al., 2019). A comparative meta-analysis of microbial functions in NHP and diverse human populations observed a comparable loss of biodiversity in captive NHP and human populations from regions with higher HDI (Manara et al., 2019), supporting previous findings (Moeller et al., 2014). However, overall, the functional characterization of NHP microbiota in previous studies has been limited

104 to only selected microbial taxa without addressing broader scale functional changes and
105 specific alterations especially in African great apes and humans. As such, robust comparative
106 functional analyses are still needed for a comprehensive understanding of how gut microbiota
107 have evolved with hominids and shaped the current structure and functional capabilities (and
108 deficits) of the human gut microbiome.
109
110 To better elucidate host-microbiome interactions in the hominid gut in an evolutionary
111 context, we present a large-scale comparative study of wild non-human apes (NHA) and
112 humans from geographically distinct populations spanning two continents. Functional
113 shotgun metagenomic sequencing was performed on feces samples of wild-living great apes
114 from six African countries, including two gorilla species, three chimpanzee subspecies, and
115 bonobos, and combined with published data from gorillas and chimpanzees from the Republic
116 of Congo (Campbell et al., 2020). Additionally, we sequenced human fecal samples from two
117 African populations (Mossoun et al., 2017) from rural villages of the Taï region in Côte d'Ivoire
118 (HDI_{2021} = 0.550; (UNDP (United Nations Development Programme), 2022)) and the Bandundu
119 region near Salonga National Park, Democratic Republic of the Congo (HDI_{2021} = 0.479), along
120 with samples from Germany (HDI_{2021} = 0.942), and included a published dataset from
121 Denmark (HDI_{2021} = 0.948; (Hansen et al., 2018)) to incorporate varying degrees of HDI. Using
122 this extensive data resource, we created a comprehensive catalog of high-quality prokaryotic
123 genomes assembled from metagenomic data, which we annotated on a taxonomic and
124 functional level. We subsequently explored patterns of diversity and host-specificity for both
125 taxonomic groups and functions, which reveals intriguing patterns associated with human gut
126 microbial communities, convergent functional adaptations across lineages, and the potential
127 mechanisms driving these patterns.
128
129 **An expanded catalog of microbial genomes from the hominid gut**
130 Using 224 shotgun metagenomic datasets (Suppl. Table S1) from fecal samples of humans
131 (Côte d'Ivoire (CIV), n=12, Dem. Rep. of the Congo (DRC), n=12, Denmark (DK), n=24, and
132 Germany (GER), n=24) and non-human apes, including two gorilla subspecies (*Gorilla gorilla*
133 *gorilla,* Gabon (GAB), n=8; *Gorilla beringei beringei,* Uganda (UGA), n=11, and Republic of
134 Congo (CG), n=28), three chimpanzee subspecies (*Pan troglodytes verus,* CIV, n=55; *P.t.*
135 *troglodytes*, GAB, n=11, and CG, n=18; *P.t. schweinfurthii*, UGA, n=12), and bonobos (*Pan*

136 *paniscus,* DRC, n=12), we reconstructed a total of 7,700 metagenome-assembled genomes
137 (MAGs) ensuring maximum completeness and low contamination using multiple binning
138 algorithms and dedicated curation and scoring tools ((Rühlemann et al., 2022); see Methods).
139 The most MAGs (quality score > 50%) were reconstructed for the most sampled subgroup of
140 great ape, *P.t. verus* (n=2,182), while the average number of reconstructed MAGs per sample
141 was the highest for *P.t. schweinfurthii* (mean=74.5). Library size / number of sequencing reads
142 was highly correlated with total assembly size ($\rho_{Spearman}$ = 0.644), which in turn was directly
143 correlated with the number of bins recovered for a sample ($\rho_{Spearman}$ = 0.966).
144
145 To ensure a comprehensive reference for the analysis, the collection of MAGs was combined
146 with two large collection of microbial reference species reconstructed from human fecal
147 metagenomes (UHGGv2, n = 4,744 isolates and MAGs; (Almeida et al., 2021)), and non-human
148 primate fecal metagenomes (n = 1,295 MAGs; (Manara et al., 2019)), resulting in a total of n
149 = 13,739 genome sequences; MAGs were subsequently clustered into 5,777 species-level
150 genome bins (SGBs; 95% ANI) using stringent criteria (Suppl. Figure S1a and S1b,
151 Supplementary Table S2). Of these, 1,074 SGBs were not previously covered by either of the
152 two large reference sets, mostly originating from NHA samples (n=956, 89.0%; Suppl. Figure
153 S1c). The highest-quality genome sequence in each SGB was chosen as its representative.
154 Overall quality of SGB representative genomes was high (median quality score = 94.1%; Suppl.
155 Figure S1d). SGB representatives were used as comprehensive reference for the estimation
156 of per-sample abundances (Methods, Suppl. Figure S1e, Suppl. Table S3). In total 3,287 SGBs,
157 encompassing 21 bacterial and two archaeal phyla (Suppl. Figure S1b), were found present in
158 the dataset. This newly curated catalog of SGBs from gorillas, bonobos, and chimpanzees
159 increases the number of microbial species genomes previously reconstructed from feces by
160 more than ten-fold, and increases mapping success of fecal metagenomes from NHAs to
161 reference genomes by two- to three-fold (Suppl. Figure S1e; (Manara et al., 2019). As
162 expected, only minor proportions of SGBs from human samples were not previously covered
163 by the included large reference collections, with 5.8%, 2.7 %, 1.8 and 1.7% of novel SGBs
164 found in samples from CIV, DRC, DK, and GER, respectively (Suppl. Figure S1e). For both NHAs
165 and humans, the highest percentages of novel diversity were observed within the phyla
166 Bacteroidota and Spirochaetota, and, to a lesser degree, within Firmicutes and Firmicutes A
167 for NHAs only (Suppl. Figure S1f). Generally, recovered clusters were highly host specific.

168 While the 7,700 MAGs spanned 1,787 of the final SGBs, only for 48 of these SGBs MAGs were
169 reconstructed from samples of more than a single host genus.
170
171 Within sample diversity varied considerably between host (sub-)species and with sequencing
172 depth (Suppl. Figure S1g). The used SGB collection covers large proportions of the diversity
173 found within the human gut (Suppl. Fig. S1e) and Faith's phylogenetic diversity (PD)
174 incorporates SGB relatedness in the diversity calculation, which enables a better estimate of
175 total diversity of a community then simpler richness estimates from taxonomic group
176 abundances. Phylogenetic diversity (PD) at an even mapping depth of 1 million reads per
177 sample showed significantly lower diversity in humans compared to all African great ape hosts
178 ($P_{Wilcoxon} = 1.2 \times 10^{-13}$; Figure 1a). Comparing individual human populations to African great
179 ape hosts revealed that humans from GER and DRC showed lower means than all NHA group
180 (all $P_{Wilcoxon} < 0.05$), while humans from CIV and DK exhibited high variance and were found to
181 have significant lower diversity than all NHA hosts ($P_{Wilcoxon} < 0.05$), except for *G. g. gorilla* and
182 *P.t. troglodytes* ($P_{Wilcoxon} > 0.05$). These two great ape taxa were found to have the lowest
183 library sizes, low numbers of recovered genomes and lowest mapping efficiency. Taken
184 together, this suggests that phylogenetic diversity in these hosts may be biased by lower
185 representation in the reference database and that the reduced diversity could be an artefact
186 of this. Consequently, samples with less than 1 million mapped reads were removed from
187 further analyses. This resulted in the removal of samples from the analysis for the groups *G.b.*
188 *beringei* (n=1), *G.g. gorilla* (n_{GAB}=5, n_{CG}=1), *P.t. troglodytes* (n_{GAB}=4), *P.t. schweinfurthii* (n=1)
189 and humans from CIV (n=1). Of note, the lowest and highest mean values for within-sample
190 phylogenetic diversity were found for the human subgroups from Germany and Denmark,
191 respectively, the latter exhibiting the only significant differences between human subsets
192 ($P_{Wilcoxon} < 0.05$ vs. DRC and GER), contradicting previous reports of lower alpha diversity
193 generally found in high HDI countries (McCall et al., 2020; Vangay et al., 2018). Additionally,
194 the considerable differences in PD observed between CIV and DRC highlight the diversity
195 found between human populations and the need to better characterize human gut
196 microbiome diversity. Therefore, while total diversity of some host groups was likely not
197 exhaustively sampled, especially considering lower abundant microbial clades, the presented
198 reference collection of high-quality metagenome reconstructed genomes likely represents
199 the current best resource for an in-depth taxonomic and functional assessment of hominid

200 fecal microbiomes and highlights that some human populations, including those sampled in
201 this analysis, have lost considerable microbial diversity in their guts.
202
203 **Phylosymbiosis in hominids is strongly supported by community structure**
204
205 Phylosymbiosis, a pattern in which microbial community divergence parallels that of the
206 hosts, can be a sign of community-level co-evolution of host and microbiota, indicative of
207 host-microbe relationships maintained over evolutionary timescales (Brooks et al., 2016). To
208 investigate such patterns, we used six different measures of beta diversity. Four were based
209 on phylogenetic or taxonomic distance metrics (weighted and unweighted UniFrac, as well as
210 genus level Aitchison and Jaccard distance), and two additional metrics considered the
211 functional capacities of the community (KEGG ortholog (KO) abundance and
212 presence/absence patterns; Suppl. Figure 2). Strong signals for phylosymbiosis were found
213 for Jaccard, and unweighted UniFrac distances ($P < 0.001$; $Q_{Bonferroni} < 0.01$), as well as a less
214 pronounced signal for Aitchison distance and the abundance of functional groups ($P < 0.01$,
215 $Q_{Bonferroni} = 0.0534$ and $Q_{Bonferroni} = 0.0585$, respectively; Figure 1b and c, Suppl. Figure 2, Suppl.
216 Table S4), but not for the distances based on presence and absence of KOs ($P = 0.055$,
217 $Q_{Bonferroni} = 0.33$) and the weighted UniFrac distance ($P = 1$). These results suggest
218 phylosymbiotic divergence in the general microbial structure of hominid microbiota (Jaccard
219 and unweighted UniFrac are based on presence/absence of microbial clades) which in part is
220 paralleled by shifted abundances of distinct taxonomic and functional groups, generally in line
221 with previous observations in other host systems (Brooks et al., 2016). This reduced signal
222 found for taxon-level diversity might be the result of fluctuating clade abundances and
223 functions in response to changing environmental factors, including diet, indicating a high
224 functional plasticity of the hominid gut microbiome in response to immediate influences,
225 while structural changes through acquisition and loss of microbial clades might rather result
226 from longer-term adaptations.
227
228 SGBs shared between host groups were analyzed in a permutation-based framework
229 accounting for differences in sequencing depth and group sizes (see Methods for details). We
230 found that especially human-associated SGBs were strongly depleted across multiple NHA
231 groups (Figure 1d), while such signal found in the opposite direction were less pronounced,
232 indicating the widespread acquisition of novel microbial clades in the human intestinal

233 microbiome. A similar pattern was found for *G. b. beringei* and multiple *Pan* subspecies,
234 however not for *G.g. gorilla*. *G.g. gorilla* and *P.t. troglodytes* are sympatric species and were
235 sampled in the same environment in the Republic of Congo and Gabon. The absence of excess
236 strong host-specific signals between these particular taxa might point towards an effects of a
237 shared environment influencing microbiome structure. Human subgroups from Europe and
238 Africa showed strong pairwise SGB-sharing between CIV and DRC, and DK and GER,
239 respectively, however not across geographic regions, suggesting strong connection of the
240 microbiome with environment and lifestyle differences. All human subgroups exhibit strong
241 depletion of SGB-sharing with all other host genera, which resulted in a clear separation of
242 the human microbiota from that of other hominids.
243
244 **Fecal microbiome of European populations marked by loss of evolutionarily conserved core**
245 **microbiota**
246
247 Abundance difference in microbial clades between humans and NHAs and between human
248 communities with differing environments, such as living in rural or urban regions, in regions
249 of the world with lower or higher HDI, can give insights into microbiome-mediated
250 adaptations to environmental changes in the distant and more recent past. We analyzed and
251 compared the abundance profiles of gut microbes between NHAs and humans, including
252 individuals living in rural, lower HDI areas of Africa (CIV and DRC) as well as individuals residing
253 in urban, higher HDI regions within Europe (GER and DK). For all following taxonomic and
254 functional comparisons, we restricted the analysis to human and *Pan* (chimpanzees and
255 bonobos) samples to obtain focused insights into the microbiota divergence since their hosts
256 diverged about 7-8 million years ago (Langergraber et al., 2012).
257
258 A total of 310 microbial genera were included in the analysis, of which 173 were found to be
259 differentially abundant ($Q_{Bonferroni}<0.05$, Figure 1d, Suppl. Table S5) in at least one of these
260 comparisons between human subgroups, or between humans and NHAs, and subsequently
261 sorted into one of four groups. We identified 57 taxa with increased abundances among
262 humans from high HDI regions in Europe, such as *Akkermansia*, *Bacteroides*, and *Alistipes*
263 (Figure 2a and b). We additionally found 39 taxa that are enriched in the two African
264 populations such as *Cryptobacteroides, Prevotella*, and *Succinivibrio* (Figure 2a and b). Overall,

265 the marker taxa of European microbiomes that we detected are in agreement with previous
266 findings (Jha et al., 2018; Pasolli et al., 2019). Our approach allowed us to identify bacterial
267 taxa that exhibit differential abundance profiles between humans and NHAs that are
268 independent from the human populations (Figure 2b). We found 74 taxa, such as *SIG603* that
269 have increased abundance in NHAs and 50 taxa with increased abundance in humans, of
270 which 15 do not show an association to either of the human subgroups, such as *Coprococcus*
271 and *Agathobacter*. Interestingly, taxa depleted in the microbiome of European individuals
272 compared to humans from Africa are more likely to be also abundant (>0.1%) in the
273 microbiomes of NHAs ($P < 0.001$; Figure 1c), suggesting a loss of evolutionary conserved
274 clades in these populations.
275
276 **Widespread changes in fecal microbiome function between hosts and across human**
277 **communities**
278 Taxon-specific changes reflect broad-scale differences between host-groups. A focused
279 analysis of microbial functions can give insights into the specific driving forces of such
280 community-level changes. We performed analysis of abundance differences of 6,340 KEGG
281 orthologs (KOs, (Kanehisa and Goto, 2000)) in NHA (genus *Pan*) vs. human fecal microbiota
282 and humans in European and African societies and found significant abundance differences
283 in 1,092 (17.2 %) and 881 (13.9 %) KOs, respectively ($Q_{Bonferroni}<0.05$; Figure 2a, Suppl. Table
284 S6).
285
286 Analysis of higher-level KEGG annotations, including e.g. complete pathways overrepresented
287 among differentially abundant KOs, revealed seven annotations with enrichment of KOs
288 higher abundant in NHAs compared to humans and nine annotations conversely enriched in
289 humans. Sulfur metabolism (map00920) was generally overrepresented in differentially
290 abundant KOs with individual effect directions associating with both groups ($Q_{Bonferroni} < 0.05$;
291 Figure 1j, Suppl. Table S7). NHA associated categories md:M00356, md:M00563
292 (methanogenesis) and path:map00680 (methane metabolism) clearly indicate a higher
293 abundance of methanogenic archaea. Additionally, we find multiple categories involving
294 ribosomes, including distinct ribosome annotations of archaea, which we could confirm using
295 the pangenome distribution of these KOs (e.g. 92.9% of SGBs with K02866 [large subunit
296 ribosomal protein L10e] belonging to the domain Archaea). In humans, we find enrichments

297 in categories covering antimicrobial resistance (path:map01501, br:ko01504), bacterial
298 mobility (path:map02030, path:map02040, br:ko02035), biofilm formation (path:map02026)
299 and prokaryotic defense systems (br:ko02048), suggesting a generally higher abundance of
300 virulence genes in human microbiomes, independent of geography. Pangenome distribution
301 of the significantly different KOs additionally confirm, these are not driven by specific
302 microbial clades since they are present across the entire phylogeny.
303
304 Enrichments of higher-level KEGG annotations between humans from Africa and Europe were
305 exclusively found for the European subgroup (n=16). These involved vitamin B_{12} / cobalamin
306 biosynthesis (md:M00122, M00924, M00925, and path:map00860) and antimicrobial
307 resistance genes (br:ko01504, path:map01502). Increased antimicrobial functions may be
308 explained by a higher use of antibiotics in human healthcare and extensive animal husbandry,
309 as well as by environmental pollution (Groussin et al., 2021). The increased abundance of
310 vitamin B_{12}-producing microorganisms in the feces of Europeans may be driven by higher
311 dietary intake of meat and dairy products from ruminants, as these food groups contain
312 microorganisms with this metabolic capacity (Watanabe and Bito, 2018). Additionally, we find
313 multiple categories suggesting a community-level shift towards oxidative carbohydrate
314 metabolism, e.g. glycolysis / gluconeogenesis (path:map00010), pyruvate metabolism
315 (path:map00620), phosphotransferase system (path:map02060), and V/A-type ATPase
316 (md:M00159).
317
318 **Success of taxa associated to European populations relates to oxidative carbohydrate**
319 **metabolism**
320
321 Community-level changes in abundances of functional groups give insights into some aspects
322 of adaptations, however, they are overproportionally driven by highly abundant taxonomic
323 groups. We applied pangenome analysis to specifically identify individual genes and functions
324 enriched or depleted within specific microbial clades overrepresented the gut of human
325 individuals residing within Europe in comparison to other human associated taxa. Analyses
326 were restricted to four bacterial families, *Bacteroidaceae, Lachnospiraceae*, *Oscillospiraceae*,
327 and *Ruminococcaceae*, for which sufficient numbers of SGBs (n>=10 in each of both groups)
328 for pangenome analysis were recovered. SGBs in these family represent large proportions of

329 the overall human microbiome (mean = 53.2%), with no significant differences between the
330 subgroups ($P_{Kruskal\text{-}Wallis}$ = 0.2). The analysis was conducted at the family-level, as higher
331 taxonomic ranks would increase clade-specific functional biases. To account for between-
332 family functional differences, functional differences of SGBs associated with Europeans were
333 first analyzed within microbial families using Fisher's exact test and subsequently subjected
334 to unweighted meta-analysis using Z-scores to leverage shared signals.
335
336 We identified 167 enriched and 30 depleted KOs in pangenomes associated with the
337 European populations ($Q_{Meta,Bonferroni}$<0.05; Suppl. Tables S8 and S9). Using higher-level KEGG
338 annotations (modules, pathways, BRITE hierarchies), we found that 11 of these annotations
339 were overrepresented in the dataset ($Q_{Bonferroni}$ < 0.05, Figure 3c, Table 1, Suppl. Table S10).
340 Among these were multiple groups involved in carbohydrate metabolism enriched in taxa
341 associated with Europeans, specifically pointing at aerobic breakdown of sugar molecules for
342 ATP generation (citrate cycle: md:M00009, path:map00020; pentose phosphate pathway:
343 md:M00004; V/A-type ATPase, prokaryote: md:M00159), confirming patterns seen also in the
344 community-level analysis of functional abundances. These signals strongly suggest that the
345 selection for taxa in the gut of humans living within Europe is connected to a diet rich in
346 carbohydrates and potentially the adaptation to transient microaerobic conditions in the gut
347 environment, using oxidative phosphorylation as a mean to release energy from nutrients,
348 which is more efficient than strictly anaerobic fermentation (Jurtshuk, 1996). However,
349 reduced fermentation can impact short-chain fatty acid production, which can, in turn,
350 potentially negatively affect the host's intestinal epithelial cells and metabolism (Deleu et al.,
351 2021). Additionally, we found a pathway connected to the histidine degradation
352 (md:M00045). Especially gut microbial histidine metabolism has been discussed with
353 relevance to human health, as it was shown that an intermediary product of histidine
354 degradation, imidazole propionate, was increased in type 2 diabetic individuals in a large
355 study of almost 2,000 individuals, and that this increase was directly connected to the
356 microbiota and overall unhealthy dietary habits, however independent of dietary histidine
357 intake (Molinaro et al., 2020). The enzyme urocanate hydratase (EC:4.2.1.49; K01712) is
358 responsible for the interconversion between urocanate and imidazole propionate in the
359 histidine degradation pathway. We find this gene significantly enriched in three of the four
360 bacterial families analyzed (P < 0.05, Figure 3d), with a clear trend visible also for

361 Oscillospiracaee (P = 0.052). This suggests a microbiome-encoded pre-disposition to
362 metabolic disorders in European human communities.
363
364 We did not find any higher-level KEGG annotations significantly enriched among the taxa not
365 enriched in Europeans. The relative lower fitness of these taxa may not result from a single
366 mechanism associated to European lifestyles, but rather from multiple selective forces
367 specific to the individual clades.
368
369 **Convergent host-specific adaptations are found across microbial families**
370 Shared gene gains or losses across multiple microbial clades can indicate a response to specific
371 host intestinal environments, leading to functions being acquired (and selected for) multiple
372 times independently. We performed a pangenome analysis of genera shared between
373 humans and NHAs (n=36) to identify such patterns of convergent adaptation. To control for
374 higher-level clade effects, functional repertoires (KEGG Ontology terms) were compared
375 between SGB pangenomes at the genus-level from NHAs (Suppl. Table S11) and humans;
376 results were then combined in a meta-analysis across genera. In total, 78 KO terms were
377 identified as carrying signatures of convergent adaptation to the respective host group, with
378 57 of these signatures associating with humans and 21 associating with NHPs ($Q_{Bonferroni}$<0.05;
379 Figure 4a, Suppl. Table S12). Among the human-associated KOs, we found multiple functional
380 groups hinting again at an adaptation to increased oxygen by utilization of oxygen as an
381 electron acceptor within the respiratory chain, such as cytochrome *bd* ubiquinol oxidase
382 subunits (cydA, cydB), as well as adaptation to increased oxidative stress through ferritin
383 (ftnA) and thioredoxin-dependent peroxiredoxin (BCP). Among the KOs enriched in NHP
384 pangenomes we found an outer membrane factor (TC.OMF), a major facilitator superfamily
385 (MFS) transporter (lrmB), 1-epi-valienol-7-phosphate kinase (acbU), and two KOs annotated
386 as polyketide synthases (rhiA, pksN). Products produced by polyketide synthases have diverse
387 functions, including antibiotic activity, virulence and support of symbiotic relationships
388 (Ridley et al., 2008). OMFs and MFS form transmembrane complexes for the transport of a
389 large variety of solutes (Yen et al., 2002), including *e.g.* carbohydrates, metal ions, amino
390 acids, and export of toxic compounds (Davidson and Chen, 2004; Lee et al., 2014). How these
391 potential adaptations relate to NHA hosts is unclear, however, they might indicate adaptation

392 to a diverse diet (Ejby et al., 2016; Tsujikawa et al., 2021) or metabolism of plant-derived
393 xenobiotics (Rodríguez-Daza et al., 2021).
394
395 *Prevotella* represented the largest genus-level clade in the dataset (n=212, 3.7% of all SGBs).
396 While we found this genus across all host species, it is largely decreased in abundance and
397 prevalence in Europeans. We selected this genus for further analysis to elucidate potential
398 functional mechanisms driving the observed patterns. Enrichment analysis revealed 126 KOs
399 with distinct prevalence patterns (Q<0.05; Figure 4b). The most striking difference was found
400 for the cytochrome *bd* ubiquinol oxidases subunits 1 and 2 (cydA and cydB), which were found
401 in 101 of 114 human-associated *Prevotella* SGBs (incl. UHGGv2 genomes), but present in only
402 two out of 72 SGBs from NHAs. It is important to note that these prevalence differences are
403 not driven by single lineages within the *Prevotella* genus that would have distribution ranges
404 restricted to single hosts. Instead, they are observed across multiple sibling clades spanning
405 the entire phylogenetic tree of the taxon (Figure 4c). Cytochrome *bd* oxidases are involved in
406 stress responses, most prominently in transiently microaerobic environments (Giuffrè et al.,
407 2014). Comparison of the *Prevotella* species tree (reconstructed using all SGB representatives
408 recovered from the dataset (n = 184)) and the cydA gene phylogeny exhibit widespread
409 incongruencies between their tree topologies (Figure 4c). We performed a tree reconciliation
410 using a duplication-transfer-loss (DTL; (Kundu and Bansal, 2018)) model between the
411 *Prevotella* and cydA phylogenies, which revealed frequent events of gene transfer ($\bar{T}$ =
412 41.552) between branches (including distant ones) of the *Prevotella* phylogeny and
413 subsequent losses ($\bar{L}$ = 23.52) in the NHA-associated clades. Interestingly, the two cydA-
414 carrying SGBs found in NHAs are phylogenetically distant, however, their cydA genes are
415 highly similar and most likely the result of a transfer from one to the other. The gene transfer
416 events and mappings were robust across 1,000 reconciliations with different starting seeds,
417 with 89.2% of all events and 67.6% of all mappings found with 100% consistency. These results
418 suggest that the enrichment of cytochrome *bd* ubiquinol oxidases observed in humans
419 compared to NHAs are the result of multiple reoccurring events of gene loss and horizontal
420 gene transfer between *Prevotella* clades within the hominid gut.
421
422 **Co-phylogeny is rare in spore-forming microbes and disrupted in humans**
423

424

425 Patterns of co-phylogeny between host and microbes can result from close interaction, or
426 even interdependence in extreme cases, and congruent metabolic pathways from co-
427 evolutionary trajectories. Using stringent selection criteria, we subjected 209 subtrees of the
428 SGB phylogeny for co-phylogeny analysis (see Methods). The subtrees spanned 46 families
429 and 945 (28.8%) SGBs present in the dataset in addition to 77 SGBs from the UHGGv2 catalog.
430 We used a Mantel-test based framework and permutation to detect co-phylogeny signals
431 ((Hommola et al., 2009), see Methods for details). When defining co-phylogeny candidates
432 based on a mean P-value < 0.05 across all permutations, 56 of 209 subtrees (26.8%) qualified
433 as exhibiting co-phylogenetic patterns (Suppl. Table S13). These subtrees cover 312 of the
434 1051 SGBs (30.7%) included in the analysis and 5.84% of the total 5,345 hominid SGBs
435 (excluding the SGBs from Manara et al.). All results and subtrees can be inspected online
436 (https://mruehlemann.shinyapps.io/great_apes_shiny_app). By visually inspecting subtrees
437 with co-phylogeny signals, we find many candidates microbial phylogenies that do not follow
438 host phylogeny, *e.g.,* in a subgroup of the genus *Cryptobacteroides* (Figure 5a). Such signals
439 suggest that co-phylogeny within the *Gorilla* and *Pan* clades can result in statistically
440 significant Mantel tests, despite topological incongruences of human-derived sequences, for
441 which no host sister (sub-)species from the same genus is available.

442

443 Human-derived genomes were found in 149 (71.3%) of the tested subtrees, of which 38
444 (25.5%) were co-phylogeny candidates. Similarly, 18 of 60 (30%) tested subtrees without
445 human-derived representatives exhibited co-phylogeny signals, *e.g.*, *W0P29-013* spp. (Figure
446 5a). Overall, 21.8% (n = 82 out of 377) of human-derived SGBs in the analysis were found in
447 co-phylogenetic subtrees, which is significantly less compared to 35.7% (n = 231 out of 647)
448 of NHA-derived SGBs ($P_{Fisher} = 2 \times 10^{-6}$). Co-phylogeny signals, defined based on the ratio of
449 SGBs in trees exhibiting co-phylogeny patterns and the total SGBs in the family included in
450 the analysis, differed strongly. Six families showed excessive signals of co-phylogeny and nine
451 families a significant depletion ($Q_{Fisher, FDR} < 0.05$; Figure 5b, Suppl. Table S14). The highest co-
452 phylogeny ratio was found for the family *Dialisteraceae* (Cophyl-Ratio = 100%, Q = 4.61 x 10^{-}
453 ^{7}), which in the analysis were entirely represented by 14 SGBs in the genus *Dialister*. *Dialister*
454 are a common, but rather neglected members of the gut microbiota which have been found
455 increased (Vals-Delgado et al., 2021; Zheng et al., 2018) and decreased (Joossens et al., 2011)

456 with various human diseases, hence their relation to human health remains unclear.
457 However, on species, *Dialister invisus,* was found to be moderately transmissible between
458 human mother-infant pairs and within households in a large meta-analysis (Valles-Colomer et
459 al., 2023). The strongest depletions were found for *e.g.* the families *Lachnospiraceae* and
460 *Treponemataceae*, the former confirming previous results for this clade (Moeller et al., 2016).
461 The latter, *Treponemataceae*, especially the genus *Treponema D,* were found depleted in
462 humans living in Europe and occur in anaerobic sediments (Thingholm et al., 2021), serving
463 as (intermediary) reservoirs for transmission to humans and NHPs, which can disrupt co-
464 phylogenetic signals by constant re-introduction to the community.
465
466 When comparing host groups, the proportion of SGBs with co-phylogeny signal is significantly
467 reduced in all human subgroups compared to the NHA hosts (all $Q_{Wilcoxon} < 0.05$; Figure 5c).
468 Further, humans from Germany and Denmark exhibited even lower proportions of co-
469 phylogeny SGBs compared to the two African human populations ($Q_{Wilcoxon} < 0.05$), but not to
470 each other ($P_{Wilcoxon} = 0.68$). The human subgroups from Africa did not differ in their co-
471 phylogeny proportions ($P_{Wilcoxon} = 0.096$). These results suggest a loss of wild great ape
472 associated clades in the intestinal microbiota of humans independent of their geographic
473 origin and the introduction of novel microbial partners with changing environment and
474 lifestyle, confirming again findings from previous analyses.
475
476 Signals of cophylogeny suggest a strong association and possible adaptation with the host and
477 the reduction of genome size and gene content are expected patterns connected to this
478 process (Toft and Andersson, 2010) which has previously been shown also for microbes with
479 codivergence patterns in human population (Suzuki et al., 2022). To explore whether these
480 processes could be detected in our dataset, we analyzed genome size and gene count, as well
481 as 43 microbial traits inferred from genome-level annotations for signals in association with
482 co-phylogeny using logistic regression, while controlling for phylogenetic relatedness (see
483 Methods; Suppl. Table S15). Out of 45 analyzed traits, 13 were found significantly depleted in
484 clades exhibiting co-phylogeny signals ($Q_{Bonferroni} < 0.05$; Figure 5d; Suppl. Table S16), including
485 genome size, gene count, capabilities to use multiple simple sugars, and bile susceptibility.
486 Phylum-level analyses confirm this overall trend especially for Actinobacteriota, Firmicutes A,
487 Firmicutes C and Verrucomicrobiota ($P_{Wilcoxon} < 0.05$), while Proteobacteria exhibited an

488 inverse signal (Figure 5d). This inverse signature might be explained by host specific
489 acquisition of genes found *e.g.* for *E. coli* across different and diverse hosts (Tiwari et al.,
490 2023), however these findings needs to be further investigated. A higher susceptibility to bile
491 in clades without co-phylogeny signal clearly suggests that bile tolerance is an adaptation to
492 the Intestinal environment of hominid hosts. The depletion of the utilization of simple dietary
493 sugars (traits: D-Xylose [Figure 5f], D-Mannose, Maltose, Glucose fermenter, Sucrose,
494 Trehalose, L-Arabinose; all Q < 0.05) in co-phylogeny clades might suggest an adaptation to
495 host-derived complex carbohydrates or other energy sources in the host-context.
496
497 Only one trait – the Arginie dihydolase pathway, also called Arginine deiminase pathway (ADI)
498 – was found enriched with co-phylogeny signal. Argninie metabolism has been widely
499 discussed in the context of host-microbe interaction (Nüse et al., 2023), and ADI specifically
500 was shown to protect bacteria from acid stress in host-association (Casiano-Colón and
501 Marquis, 1988), but was also shown to modulate host immunity (Ghazisaeedi et al., 2022)
502 and as specifically acquired by Saccharibacteria in the process of colonization of mammals
503 (Tian et al., 2022), confirming its potential association with co-phylogeny in hominids.
504 Previous analyses suggested that spore-forming clades are less likely to be exhibiting co-
505 phylogenic patterns, due to their ability to survive outside of the gut, facilitating dispersal
506 between hosts (Groussin et al., 2020; Hildebrand et al., 2021; Moeller et al., 2016; Nayfach et
507 al., 2016). We did not find any negative correlation between spore-formation ability and co-
508 phylogeny patterns (Q = 1, Suppl. Table S16), however the annotation of this trait was
509 restricted to only two phyla (Firmicutes and Firmicutes A) and was also rare within these
510 clades, being found in only 54 SGBs across the dataset. As such, whether these results
511 contradict previous findings cannot be concluded in this analysis and warrants future focused
512 analyses.
513
514 We found 67 out of 157 SGBs in *Bacteroidaceae* within subtrees with cophylogeny signals (Co-
515 pylogeny-Ratio = 43.5%), consistent with previous findings based on *gyrB* amplicon data
516 (Moeller et al., 2016). However, no evidence for strict co-phylogeny was found in
517 *Bifidobacteriaceae* (n_{SGB}=10 in the analysis, none with co-pyhlogeny signals), which is
518 inconsistent with findings from the same report (Moeller et al., 2016). Comparing the
519 phylogeny of metagenome-derived *gyrB* sequences and the GTDB marker-gene phylogeny for

520 *Bifidobacterium spp.* revealed clear incongruences between both approaches (Figure 5g),
521 which may explain the differences in the presented analysis and previous findings.
522
523 **Discussion**
524 Here, we present the largest curated dataset of fecal metagenomes derived from wild African
525 great apes and human populations. For this, we surveyed and reconstructed high-quality
526 microbial genomes from the feces wild non-human apes, including gorillas (*Gorilla gorilla*
527 *gorilla*; *Gorilla beringei beringei*), chimpanzees (*Pan troglodytes verus*; *P.t. troglodytes*; *P.t.*
528 *schweinfurthii*), and bonobos (*Pan paniscus*) as well as human populations from Africa and
529 Europe. We identified signals of phylosymbiosis across the included hominids, indicating a
530 conserved evolutionary relationship of microbial communities with their host species.
531 Moreover, by employing a comparative approach, we found extensive changes of microbial
532 taxonomic and functional abundances across the intestinal microbiota of NHAs and humans.
533 Previous studies have pointed to "Western" lifestyles as an important factor influencing the
534 intestinal microbiota in humans. Within our human sample population, we were able to
535 confirm differential signals of prokaryotes associated with the European human populations.
536 Importantly, using a comparative dataset of great ape taxa showed that microbial clades lost
537 in Europeans in comparison to African human populations are also found in wild great ape
538 populations. Thus, we suggest that the loss of these taxa might be regarded as the departure
539 from a natural divergence trajectory since their last shared ancestor, cumulating in a mass
540 extinction event of evolutionary conserved members of hominid-associated gut microbiota.
541 While it is tempting to link these changes to industrialization (as previous studies have done),
542 there are many differences between these human populations (e.g., genomic diversity, diet,
543 exercise, sunlight exposure, exposure to antibiotics, population bottlenecks) and it was
544 certainly not possible with the sampling regime here, to determine the particular factors
545 responsible for the variation observed between the human populations sampled here. Due
546 to logistic constraints, preservation methods for fecal samples from the included hosts and
547 host subgroups differ. While these are expected to influence microbiome composition,
548 previous studies show that individual signature are retained independent of storage methods
549 (Blekhman et al., 2016). Despite this caveat, that fact that considerable variation exists
550 between human populations is notable and highlights the need for much higher resolution
551 sampling of human associated microbial diversity. Similarly, our analysis suggests that there

552 is even more undescribed microbial diversity to be discovered across populations of wild non-
553 human apes.
554
555 In a pangenome analysis to identify individual genes or functions enriched or depleted in
556 genomes of taxa associated with different human populations, we identified numerous
557 functional traits involved in aerobic respiration associated with the European populations in
558 the analysis. We hypothesize that taxa found to be enriched in the fecal samples of humans
559 from Germany and Denmark might have a selective advantage via their clade-independent
560 ability to survive or even utilize aerobic conditions in the intestinal tract. More specifically,
561 we propose that these taxa have undergone convergent adaptation to tolerate high oxygen
562 concentrations. Such aerotolerance could increase microbial fitness, whereby bacteria can
563 withstand high oxygen concentrations to metabolize mucus layers for energy (Zheng et al.,
564 2015). However, the depletion of this mucus by bacteria diminishes an important physical and
565 immunological barrier that protects the human host against microbial assaults and allows for
566 direct interaction between host epithelial cells and microbiota, potentially triggering (auto-
567)immune processes (Costa et al., 2016; Matute et al., 2023). Notably, we showed that the
568 introduction of novel microbes associated with industrialization related to vast differences in
569 the community composition of fecal microbiota in the European populations. Thus, it is
570 possible that susceptibility to intestinal inflammation might be potentiated by specific taxa
571 found in this population. Accordingly, we found increased abundances of well-characterized
572 mucin-degrading taxa, including *Akkermansia* and *Bacteroides*, in the European cohorts.
573 These findings are congruent with previous reports suggesting that there is increased mucus
574 degradation by intestinal microbiota in human populations with direct access to industrial
575 food systems, which may relate to higher incidences of inflammatory bowels diseases
576 observed in developed economies (E. D. Sonnenburg and Sonnenburg, 2019).
577
578 Comparatively, only a few pathways showed conserved enrichment in the opposite direction,
579 suggesting clade specific mechanisms for their loss in some human societies. In particular, we
580 found the taxon *Prevotella* is depleted in German and Danish samples but conserved across
581 hominids, despite representing a diversity of host clades and diets. *Prevotella* is a major
582 determining taxon of one of the human enterotypes, a concept used to define fecal microbial
583 communities (Arumugam et al., 2011). It remains controversial as to whether the human gut

584 microbiome is best classified using such discrete categories, or rather along a dynamic,
585 continuous gradient (Cheng 2019, Knight 2014). Nevertheless, previous reports have shown
586 that individuals who access industrialized food systems (i.e., consume so-called
587 "Westernized" diets) generally display a *Bacteroides*-dominant enterotype. *Bacteroides*-
588 enterotypes have been previously associated with a multitude of intestinal (Vieira-Silva et al.,
589 2019) and extra-intestinal inflammatory diseases (Valles-Colomer et al., 2019). Conversely,
590 individuals who rely on rural and traditional subsistence strategies (i.e., consume plant-rich
591 diets) tend to exhibit a *Prevotella*-dominant enterotype (Vangay et al., 2018). This enterotype
592 is also displayed in about 20% of individuals living within Western societies (Costea et al.,
593 2018). Interestingly, there are conflicting reports concerning *Prevotella* and host health.
594 While it has been shown that *Prevotella* may improve glucose metabolism (Kovatcheva-
595 Datchary et al., 2015), other reports have linked high abundances of *Prevotella* spp. with
596 autoimmune diseases and intestinal inflammation (Iljazovic et al., 2021). While results from
597 model systems have suggested *Prevotella* likely plays a role in autoimmunity, these studies
598 largely relied on mono-colonization of germ-free animals and thus may be biased due to a
599 lack of microbial interaction partners and an aberrant host physiology (Iljazovic et al., 2021).
600 Within human studies, no convincing link between increased *Prevotella* spp. and
601 inflammatory bowel disease has yet been shown (Iljazovic et al., 2021).
602
603 Here, we used an evolutionarily-informed framework to extend the enterotype concept to
604 elucidate the functional dynamics involved in the assembly of the human gut microbiome
605 over evolutionary timescales. Such insights may better inform how changes in the gut
606 microbiome might affect human health. We find the taxon *Prevotella* to be conserved across
607 the sampled hominids. Moreover, the sheer diversity of *Prevotella* displayed across all
608 hominid clades clearly suggests an evolutionary conservation and long-standing interaction
609 of this microbial clade with the host, as further revealed by host-specific microbial functions
610 identified in the metagenomic pangenome analysis. In other words, we find the *Prevotella*
611 clade to be an integral member of the intestinal microbial community of all hominids.
612 Therefore, we propose that the *Prevotella*-enterotype represents an evolutionary ancestral
613 community state for the human gut microbiome. Rather than a discrete enterotype, a
614 reduced abundance and diversity of *Prevotella* may better regarded a key biomarker for
615 disease risk (Gorvitovskaia et al., 2016) or for microbiota insufficiency syndrome (J. L.

616 Sonnenburg and Sonnenburg, 2019), which seems to be partly driven by changes associated
617 with Western lifestyles. Additional research and large-scale strain collections for *Prevotella*
618 are needed for an in-depth analysis and evaluation of this diverse taxonomic group with
619 regard to host health and its role in inflammation. Such research must consider *Prevotella*
620 *spp.* as members of a complex consortium of interacting microorganisms and as, we argue, a
621 potential target for pre- and probiotic intervention in chronic inflammatory disorders.
622
623 Lastly, we leveraged our catalog of high-quality metagenome-assembled genomes from
624 hominid fecal samples together with existing data to investigate co-phylogenetic patterns
625 across the sampled hosts. Overall, co-phylogeny showed highly clade-specific enrichments
626 and depletions. In addition, human-derived MAGs were found significantly less often among
627 co-phylogenetic groups than MAGs from NHAs. Since we included human-derived data from
628 global reference datasets (Almeida et al., 2021), this effect is unlikely to be an artifact of non-
629 exhaustive coverage of human microbiome members. We found several microbial traits
630 depleted among bacteria with cophylogenetic patterns. Among these were, as expected,
631 reduced genome sizes and gene counts, as well as susceptibility to bile and utilization of
632 multiple simple carbohydrates. We hypothesize that these depletions mirror the
633 specialization of microbes to colonize the hominid gut and utilize host-derived complex
634 carbohydrates.
635
636 Our study has limitations. The co-phylogeny analysis relies heavily on genome-sequences
637 recovered from shotgun metagenomic sequencing (MAGs), which are potentially
638 contaminated and incomplete, which could bias tree structure and thus, co-phylogeny
639 estimates, and also the can potentially under- (or over-)estimate the functional capacities of
640 recovered microbial genomes. To address the potential shortcomings of MAGs, we
641 implemented stringent data processing pipelines and quality control to achieve the high-
642 quality MAGs and a host-specific pan-genome based functional annotation framework
643 incorporating information from multiple MAGs per species representative to reduce potential
644 genome gaps (see Methods). Additionally, the commonly used estimates of divergence times
645 of the hominid hosts included in the analysis set the timeframe of the split from a shared
646 ancestor to 8-19 million years ago (Langergraber et al., 2012; Scally et al., 2012). Bacterial
647 speciation events happen in the timeframe of 10-100 million years, or longer (Marin et al.,

648 2017; McDonald and Currie, 2017; Ochman et al., 1999), and thus, co-phylogeny in hominids
649 is expected to be observed within microbial species or possibly genera. In the presented
650 dataset, species-level sharing of MAGs between host genera was low (1.68%; n = 30 out of
651 1,787 reconstructed SGBs, not including Manara *et al*. and UHGGv2). SGBs were defined on
652 95% average nucleotide identity, a measure generally regarded as appropriate (Jain et al.,
653 2018), but it is nevertheless prone to clade specific biases, potentially further influenced by
654 altered speciation dynamics in association with (evolutionary) changes in host lifestyle
655 (Lawrence and Retchless, 2009), *i.e.* previously demonstrated increases in horizontal gene
656 transfer (HGT) within individual microbiomes (Groussin et al., 2021). Accounting for these
657 potential biases, we relaxed the threshold to a shared genus-level annotations for subgroups
658 to be included in the co-phylogeny testing, while keeping the number of tested sub-
659 phylogenies to a minimum through the definition of stringent inclusion criteria (see Methods).
660 Despite these considerations, the observation of signals of co-phylogeny across hominids is
661 supported by a robust statistical framework.
662
663 Additional limitations stem from the focus on humans and African great apes. While the
664 comparisons between these host-clades provide a framework for the in-depth investigation
665 of (evolutionary) rather recent adaptations and between-host divergences, they potentially
666 neglect that could be revealed by broader-scale investigations, such as the previously
667 described convergence of the human gut microbiota towards that of cercopithecines (Amato
668 et al., 2019). However, our analyses show the impact of the unique trajectories taken by the
669 intestinal microbiomes of *Pan* and *Homo* since their last common ancestor.
670
671 Our work here lays the foundation for the analysis of disease-associated changes in the
672 human intestinal microbiome in an evolutionarily informed framework, thereby allowing
673 researchers to evaluate microbiome-associated inflammatory disorders from a point of view
674 that considers both proximal and evolutionary influences. Future investigations should
675 consider in-depth analysis of horizontal gene transfer events within or even between primate
676 hosts to shed further light on also cross-species dynamics and transition of microbes. Such
677 analyses however require either microbial isolate genomes or at least long-read sequencing
678 data to increase confidence in detection events. Additionally, time series data for host groups
679 sharing the same habitat, *e.g. G. g. gorilla* and *P. t. troglodytes*, could give additional insights

680 into cross-species sharing dynamics which cannot be appropriately elucidated based on
681 single-timepoint data.
682
683 In summary, we present an in-depth taxonomic and functional description and analysis of
684 hominid-associated fecal communities spanning about ten million of years of evolution and
685 host-microbiome interactions in the gut of humans and African great apes. Western lifestyle
686 and maybe more precisely industrialization associated changes in human gut microbiota have
687 been previously suggested as a driver of microbiome insufficiency syndrome, whereby an
688 incompatibility between quickly adapting microbiota and slowly evolving host genes leads to
689 chronic inflammatory diseases such as metabolic syndrome, type 2 diabetes, and
690 inflammatory bowel disease (E. D. Sonnenburg and Sonnenburg, 2019; Wallenborn and
691 Vonaesch, 2022). Thus, a comparative analysis of human and NHA intestinal microbiota that
692 considers evolutionary forces as presented herein provides a powerful platform to advance
693 our understanding of human-associated microbiota and guide the development of
694 personalized, targeted interventions to prevent and treat chronic inflammatory disorders.
695

Methods

Ethics & Inclusion statement

Ethical approval for work on human samples was obtained from the Local Ethics Committee Germany, Kiel (reference number A156/03), the Ivorian ethics commission (Comité national d'éthique et de la recherche [CNER], permit number 101 10/MSHP/CNER/P) and the Congolese ethics commission (Comité d'Éthique, Ministère de l'Enseignement Supérieur et Universiaire, permit number ESO/CE/018/11). All procedures performed in studies involving human participants were in accordance with the ethical standards of the institutional and/or national research committee and with the 1975 Helsinki declaration and its later amendments or comparable ethical standards. Sampling of wild-living great apes and human populations in Africa were granted by: Bwindi Impenetrable Forest National Park, Uganda (*Gorilla beringei beringi, Pan troglodytes schweinfurthii*): the Uganda National Council for Science and Technology and the Uganda Wildlife Authority; Kokolopori Bonobo Reserve and Bandundu region, Democratic Republic of the Congo (*Pan paniscus,* Human): the Ministere de Recherche Scientifique et Technologie, Democratic Republic of the Congo; Loango National Park, Gabon (*Gorilla gorilla gorilla, Pan troglodytes troglodytes*): the Agence Nationale des Parcs Nationaux, the Centre National de la Recherche Scientifique et Technique of Gabon; Taï National Park and region, Côte d'Ivoire (*Pan troglodytes verus*, Human): the Ministère de l'Enseignement Supérieur et de la Recherche Scientifique, the Ministère des Eaux et Fôrets in Côte d'Ivoire, and the Office Ivoirien des Parcs et Réserves. Researchers from CIV and DRC contributing to the conducted research and fulfilling the authorship criteria were included as co-authors. Research at sites in Africa was conducted in collaboration with local partners as stated in the acknowledgements section, granted by local authorities and in agreement with local policies. Feces from wild-living, habituated animals were collected after defecation without interfering with the animals. Research at great ape sites was increasingly performed following the IUCN guidelines to minimize disease risk for great apes. We did not stratify or correct for sex or gender effects in the analysis. Our analyses focus on the comparison of gut metagenomes from either distinct hominid species or between human subgroups from populations with differences in human development index. We expect that the effects of sex and/or gender are negligible in this context and these factors have not been explored in the current analysis.

728 **Fecal Sampling, DNA extraction and data generation**

729 Sampling of wild-living great apes and human populations in Africa were conducted at: Bwindi
730 Impenetrable Forest National Park, Uganda (*Gorilla beringei beringi, Pan troglodytes*
731 *schweinfurthii*); Kokolopori Bonobo Reserve and villages adjacent to Salonga-Sud National
732 Park, Democratic Republic of the Congo (*Pan paniscus,* Human); Loango National Park, Gabon
733 (*Gorilla gorilla gorilla, Pan troglodytes troglodytes*); Taï National Park and adjacent villages,
734 Côte d'Ivoire (*Pan troglodytes verus*, Human). Sampling procedures for collecting feces from
735 humans (n=48) and wild non-human primates (n=109) have been previously described
736 (Gogarten et al., 2021). Briefly, fecal samples were collected immediately after defecation,
737 and, depending on the local infrastructure, either stored in RNAlater and frozen at -20°C or
738 stored in a cryotube, cooled in a thermos until return to the field laboratory, and subsequently
739 snap frozen in liquid nitrogen. Appropriate government permits and permission to conduct
740 research on wild primates were granted by the relevant authorities (see Acknowledgments
741 for site-specific details). Human fecal samples from the Democratic Republic of Congo (n = 12)
742 were stored in RNAlater and frozen at -20°C. Human fecal samples from Côte d'Ivoire (n=12)
743 were stored in a cryotube, cooled in a thermos until return to the field laboratory and
744 subsequently snap frozen in liquid nitrogen. Human fecal samples from Germany were
745 collected at home by the participant in standard fecal collection tubes, mailed to the study
746 center, and stored at -80°C. DNA extraction from fecal samples was performed from 200mg
747 of stool transferred to 0.70mm Garnet Bead tubes (Qiagen) with 1.1 mL ASL buffer, followed
748 by bead beating in a SpeedMill PLUS (Analytik Jena AG) for 45 s at 50 Hz. Samples were heated
749 to 95°C for 5 min and centrifuged, retaining 200 µl of the supernatant for DNA extraction with
750 the QIAamp DNA Stool Mini Kit (Qiagen) automated on a QIAcube system (Qiagen) according
751 to the manufacturer's protocol. DNA quality was assessed by Qubit and Genomic DNA
752 ScreenTape (Agilent). Illumina Nextera DNA Library Preparation Kit was used to construct
753 shotgun metagenomic libraries, and subsequently sequenced with either 2 × 125 bp reads on
754 a HiSeq 2500 platform or with 2 × 150 bp reads on a NovaSeq 4000 machine (Illumina).

755

756

757 **Data processing, assembly and metagenomic binning**

758 Raw sequencing FastQ files were quality controlled and preprocessed using the BBMap
759 software suite ("BBMap," n.d.). Host reads were removed using bbmap.sh. A masked human

760 reference database ("Introducing RemoveHuman," 2014) and a lenient mapping threshold of
761 95% identity was used to account for a broader host range to also capture host contamination
762 from the *Pan* and *Gorilla* host. Metagenomic contigs were assembled with metaSPAdes and
763 contigs >= 2000 bp were retained (Bankevich et al., 2012). Reads were mapped to the contigs
764 of the respective samples using Minimap2 (Li, 2018), converted to BAM files with Samtools
765 (Li et al., 2009) and used to estimate per-contig mapping depth with the
766 jgi_summarize_bam_contig__depths binary from the MetaBAT2 binning tool (Kang et al.,
767 2019). Contig binning for individual samples was performed with MetaBAT2 (Kang et al.,
768 2019), MaxBin2 (Wu et al., 2016) and CONCOCT (Alneberg et al., 2014). In addition, the VAMB
769 binning tool (Nissen et al., 2021) was used on a cross-mapping catalog of the merged contigs
770 from all samples within each host group. Individual binning results were refined using
771 MAGScoT (Rühlemann et al., 2022) to acquire high quality metagenome-assembled genomes
772 (MAGs) for each sample. Clustering of MAGs to species-level genome bins (SGBs) was
773 performed with dRep (Olm et al., 2017) in a multi-step approach to control for inflated SGBs
774 due to low MAG quality. First, MAGs were dereplicated to 97% similarity within each host
775 group, choosing the MAG with the highest score (calculated by MAGScoT based on
776 completeness and contamination) as cluster representative. High and good quality
777 representatives (score > =0.7) from all host groups together with representative sequences
778 from the UHGG v2 were then clustered into 95% SGBs using dRep, again selecting the highest
779 quality MAG as representatives. Medium quality (scores between 0.5 and 0.7) 97%
780 representatives from previous clustering step were then compared to SGB representatives
781 using fastANI (Jain et al., 2018), assigning MAGs with high similarity (>=95%) to the respective
782 SGB. Medium quality 97% representatives without hits to the high quality SGB library were
783 then clustered into 95% SGBs and added to the catalog in the case of at least two genomes in
784 the cluster, discarding singleton clusters. The final catalog of SGB representatives was used
785 to quantify contig abundances in all samples using Salmon in metagenome mode (Patro et al.,
786 2017). Taxonomic annotations were performed using the GTDBtk (v2.1) and GTDB release
787 207v2 (Chaumeil et al., 2022; Parks et al., 2022). For SGBs without genus- and/or species-level
788 assignments, the SGB ID was used as taxonomic label. GTDBtk marker gene alignments were
789 used to generate a phylogenetic tree of all SGB representatives using the respective "infer"
790 function of the GTDBtk. All data processing scripts are available online:
791 https://github.com/mruehlemann/greatapes_mgx_scripts

792

793 **Pangenome catalog creation, annotation and analysis**

794 All MAGs underwent calling of coding sequences using prodigal (v2.6.3) (Hyatt et al., 2010).
795 Protein sequences were clustered based on 95% similarity using MMseqs (Hauser et al., 2016;
796 Steinegger and Söding, 2017) and annotated using the emapper.py script of the eggNOG-
797 mapper v2 (Cantalapiedra et al., 2021) annotation tool with the eggNOG 5.0 reference
798 database (Huerta-Cepas et al., 2019). MAG level functional profiles based on KEGG Ortholog
799 annotations were collapsed into SGB-level pangenomes for each host genus (*Homo, Gorilla*,
800 and *Pan*). In the case that no MAGs of an SGB were recovered from a given host genus,
801 functional profiles were inferred from MAGs across the other host groups, accounting for
802 host-specificities in the inferred accessory genomes/functions by considering a function to be
803 present if it was present in all host-specific pangenomes of the respective SGB with MAGs
804 recovered from the metagenomic data.

805

806 **Calculation of microbial clade and functional abundances**

807 All downstream data processing and statistical calculations were performed in R v4.2 (R Core
808 Team, 2022) and using the tidyverse library (Wickham et al., 2019). Per-sample contig
809 abundances for the SGB representatives from Salmon were used to estimate SGB
810 abundances. Salmon output includes total mapped reads per contig and mapping reads
811 adjusted for library size and total sequencing depth as transcripts per million (TPM), a
812 measure from the transcriptomics field which can be directly transferred to metagenomic
813 libraries. Individual contig coverages were calculated from the number of mapped reads and
814 the effective lengths of the Salmon mapping output, considering contigs with > 10% coverage
815 as present. An SGB was considered present when at least 20% of its total length was in contigs
816 marked as "present" and if at least 1,000 total reads and 250 TPM mapped to it. Final SGB
817 abundances were calculated as TPM, calculated from the reads mapping to the SGBs present
818 in the respective sample, thus representing a normalized abundance across all samples.
819 Combining SGB abundances with taxonomic assignments, domain- to species-level
820 abundances were calculated as cumulative TPM abundances within the respective taxonomic
821 bins. Rarefactions were calculated based on 5-fold repeated subsampling of contig level
822 mapped reads at 100k, 250k, 500k, 1M, 2.5M, 5M, and 10M reads, followed by TPM
823 calculations as described above. By rarefying reads and not TPM we realistically simulate

824 sampling effects introduced by low coverage and low abundances of SGBs affecting especially
825 samples with small library sizes. Community level functional profiles were calculated be
826 multiplying TPM abundances of SGBs with the respective host-genus specific functional
827 profiles (presence of KEGG orthologs [KOs]) of the SGBs and summarizing the per-SGB values
828 into a sample-level abundance of functional annotations. Ultimately, functional abundances
829 of individual KOs represent the cumulative TPM abundance of SGBs carrying the respective
830 KO.
831
832 **Alpha and beta diversity**
833 Faith's phylogenetic diversity (PD) (Faith, 1992) was used as measure of alpha diversity,
834 calculated from the phylogenetic tree based on GTDBtk marker genes using the pd() function
835 of the picante package for R (Kembel et al., 2010). Genus-level increase of PD from novel SGBs
836 was calculated from the differences of PDs with and without novel SGB annotated as the
837 respective genus. Sample level PDs were calculated from the SGB presence/absence patterns.
838 Beta diversity was assessed as unweighted and weighted UniFrac distances (Lozupone et al.,
839 2011) using the UniFrac() function of the phyloseq package for R (McMurdie and Holmes,
840 2013) and SGB abundances and the phylogenetic tree based on GTDBtk marker genes as
841 input. Aitchison distance (Aitchison, 1982) was calculated from the CLR-transformed genus-
842 level TPM abundances obtained from the clr() function from the compositions package for R
843 (van den Boogaart and Tolosana-Delgado, 2008) and adding a pseudocount of 1 to all
844 abundances, setting all CLR-transformed abundances below zero to zero. Jaccard distances
845 (Jaccard, 1912) were also calculated on genus-level presence/absence patterns using the
846 vegdist() function from the vegan package for R (Oksanen et al., 2022). Genus-level
847 abundances were chosen for Aitchison and Jaccard distance, as SGBs are highly host-specific,
848 thus would lead to high beta-diversities simply due to host exclusive SGBs, grouping at genus-
849 level prevents from this and UniFrac distances use phylogenetic relations between SGBs.
850 Beta-diversity on functional abundances were calculated from the Euclidian distances of the
851 log-transformed KO abundances adding a pseudocount of 1 to avoid undefined values.
852 Presence-absence values of KOs were treated in the same way as described above and using
853 Jaccard distance to infer pairwise distances.
854
855 **Cross-host sharing analysis**

856 Permutation-based analysis of excessive and reduced sharing of SGBs between host groups
857 were based on the mean SGB abundances of the five rarefaction of 1M mapped reads to
858 account for differences in library depth impacting SGB richness and per-group sample sizes.
859 For each host group, 100-fold sampling of five samples from this group were drawn and the
860 SGBs found in the host were analyzed for their presence in five random samples of each of
861 the other host groups, calculating the relative amount of shared SGBs as $Rel_{shared} = n_{SGB,shared}$
862 $/ n_{SGB,host}$. The mean of all 100 samplings was used as relative sharing coefficient for all host
863 pairs in both directions. Excess and reduced sharing was analyzed by 1000-fold drawing of
864 five random samples accounting for differences of host groups and the repetition of above
865 calculations for relative sharing with all host groups. P-values were calculated from the
866 proportions of random samplings exceeding/falling below the true sharing coefficients.
867
868 **Phylosymbiosis analysis**
869 Phylosymbiosis was assessed using five measures for community level diversity, unweighted
870 and weighted UniFrac, genus-level Aitchison, and Jaccard distances, as well as KEGG ortholog
871 (KO) abundance based Aitchison distance, and following the approach described in Brooks et
872 al. (2016). Briefly, host group differences were used to infer microbiome dendrograms by
873 UPGMA clustering. Branch support was calculated from 1000-fold jackknife sampling.
874 Robinson-Foulds distances between microbiome trees and host phylogeny were calculated
875 using the RF.dist() function from the phangorn package for R (Schliep, 2011). Significance of
876 phylosymbiosis was assessed using the host phylogeny and 100,000 random trees as
877 comparison for the microbiome trees. Tanglegrams were created with the ggtree and cowplot
878 packages for R (Yu et al., 2017).
879
880 **Assessment of between-group abundance differences**
881 Taxonomic abundance differences between Humans and NHAs, as well as between humans
882 living outside and within industrialized systems were based on CLR-transformed abundances
883 to account for the compositionality of microbiome data (Gloor et al., 2017). Included in the
884 calculations were all genera with a prevalence > 20% and relative abundance (before CLR-
885 transformation) of > 0.1% in at least of the host groups and all KO abundances with a
886 prevalence > 20% and CLR-transformed abundance of > 1 in at least one of the host groups.

887 KO abundances were filtered accordingly and subsequently (log+1)-transformed to achieve a
888 less skewed distribution. Log-transformation was chosen, as CLR-transformation assumes
889 compositionality of the data, which is – unlike for taxonomic abundances - not fulfilled for
890 functional abundances. Abundance differences were assessed in a linear regression in R (R
891 Core Team, 2022) using abundances as dependent variable and human/NHA and
892 European/African dichotomies as explanatory variables in a single model for each taxon (or
893 function), assessing associations with all groups at once, the model was defined as
894 lm(abundance ~ Human + European). P-values were calculated from the t-values of the
895 resulting models using the summary.lm() function. Log-fold differences were calculated using
896 group mean abundances and a pseudocount of 0.01. P-values were adjusted for multiple
897 testing using Bonferroni correction. Features with significant ($Q < 0.05$) positive association
898 with NHAs were grouped as "NHA associated". Features associating with geographic
899 differences (Europe/Africa) were grouped into the respective group they were positively
900 associated with. Remaining genera with significant differences between humans and NHAs,
901 but not with a particular subgroup were grouped as "human associated". Genera without
902 abundance differences in any of these comparisons were grouped as "unchanged" or "other".
903
904 **Functional pangenome differences between groups**
905 Pangenome catalogs of human-associated SGBs were compared within microbial families
906 between SGBs in taxonomic groups found enriched in European communities compared to
907 other human-associated taxa, independent of a strong association with geography. KEGG
908 Ontology (KO) term annotations were used as functional groups and their prevalence
909 differences between groups were assessed using Fisher's exact test. Per-family effect sizes (Z-
910 Scores) of KOs were calculated from P_{Fisher}-values and the direction of the effects which were
911 assessed using the log2 of the ratio of prevalences in the two groups and a pseudo count of
912 0.01. The sum of the Z-Scores were added and divided by the square-root of the total number
913 of families the respective KOs were found in to obtain a Z_{Meta} for each KO term, used to
914 calculated P_{Meta}. P_{Meta}-values were adjusted for multiple testing using Holm-correction. KO
915 terms with $Q < 0.05$ and present in at least two of the microbial families in the analysis were
916 considered as functions with differential prevalence. A similar approach was employed to
917 assess functional differences between NHP- and Human-associated SGBs, however in this
918 case, SGB pangenome differences were compared on genus level and the meta-analysis was

919 performed combining signals from all genera, and specifically across the genera within
920 particular phyla.
921
922 **Tree reconciliation analysis**
923 Proteins from the representative SGBs of the genus *Prevotella* annotated with the annotation
924 "cydA" (cytochrome *bd* oxidase subunit 1) as "Preferred name" in the emapper/eggNOG
925 annotation were extracted from the unclustered protein sequence catalog. The same
926 procedure was followed for *Paraprevotella clara,* which was included as an outgroup.
927 Incomplete cydA sequences were removed using a length threshold of 200. Protein sequences
928 were aligned using Clustal Omega (Sievers et al., 2011). The alignment was used to
929 reconstruct the phylogenetic tree using IQTREE2 (Minh et al., 2020) and a automatic model
930 selection, which resulted in an LG+F+R8 model to be chosen as best-fit model according to
931 the Bayesian information criterion (BIC). Branch support values were calculated using UFBoot
932 (Minh et al., 2013) and performing SH-aLRT test (Guindon et al., 2010). Alignments of GTDBtk
933 marker protein sequences for *Prevotella* SGBs and *Paraprevotella clara* were used to
934 reconstruct a genome-level species phylogeny in the same respective way as described above
935 for the cydA sequences (BIC best-fit: LG+I+I+R5). Very low confident branches (< 60%
936 bootstrap support) in the cydA phylogeny were resolved together with the species tree using
937 the OptResolutions supplementary program of the RANGER-DTL 2.0 software (Bansal et al.,
938 2018) resulting in 495 equally probable trees with optimized duplication-transfer-loss costs
939 using default values (duplication: 2, loss: 1, transfer: 3). A randomly chosen output tree was
940 using in the reconciliation analysis with the species tree in RANGER-DTL 2.0 using default
941 values and 1,000 random starting seeds in parallel (Tange, 2011) to assess robustness.
942 Resulting sampling outcomes were summarized using the AggregateRanger tool of the
943 RANGER-DTL 2.0 software package.
944
945 **Co-phylogeny analysis**
946 Host phylogenetic trees were obtained from the 10kTrees website ((Arnold et al., 2010);
947 https://10ktrees.nunn-lab.org/). To assure high quality microbial phylogenies for the co-
948 phylogeny analysis, family-level maximum-likelihood trees were reconstructed from the
949 GTDBtk marker gene alignments with the IQTREE2 software (Minh et al., 2020) and a WAG
950 model including a random SGB outside the respective families as outgroups. Family level trees

951 were rooted and for each SGB traced from tip to root to identify for each SGB the smallest
952 subtree which covered 4, 5, 6, and 7 host groups. Combining information from all SGBs, the
953 overall set of smallest trees to be included in the co-phylogeny analysis were identified,
954 discarding subtrees for which the inclusion criterion was fulfilled already for a smaller tree
955 starting from a different tip. In addition, subtrees spanning more than a single genus were
956 excluded from the analysis, as divergence times of microbial genera predate divergence of
957 the included hosts (Ochman et al., 1999). For all subgroups included in the analysis,
958 maximum-likelihood distances and trees using a WAG model in IQTREE2 were inferred from
959 the marker gene alignment of all MAGs assigned to the SGBs in the respective subgroups. Co-
960 phylogeny of the subgroup was assessed by randomly selecting one MAG per host, calculating
961 congruence with the host tree by Robinson-Foulds metric and by Mantel-test (Hommola et
962 al., 2009). Tiplabels were permutated 999-fold and P-values calculated. This process starting
963 from the random selection of one MAG per host was repeated 999 times to obtain final P-
964 values. Family-level co-phylogeny ratios were calculated based on the ratio of SGBs within
965 subtrees with co-phylogeny signal and total SGBs in the respective family that were included
966 in the analysis. Enrichment of co-phylogeny for each microbial family was calculated by using
967 Fisher's exact test on the SGBs in the analysis dividing them into four groups based on family
968 membership and being in a subtree with co-phylogeny signal. All P-values were adjusted using
969 FDR correction.
970
971 **Correlation of microbial phenotypes with cophylogeny signals**
972 SGB representative genome sequences were analyzed using the Traitar tool (Weimann et al.,
973 2016) to infer up to 67 microbial traits. A total of 43 inferred traits present in more than 50
974 and less than 1017-50 = 967 of the 1,017 SGBs included in the cophylogeny analysis were
975 analyzed for their association with cophylogeny signals. Using the R package lme4qtl
976 (Ziyatdinov et al., 2018), for each of the traits a mixed logistic regression model was fitted
977 across for the 1,017 SGBs, using signal of cophylogeny (binary trait) as dependent variable
978 and the trait as bineray fixed effect explanatory variable, accounting for phylogenetic and
979 taxonomic relatedness between SGBs by including a relatedness matrix and phylum-level
980 categories as random effects in the model and using a binomal function with probit as link.
981 The relationship matrix was calculated by using the cophenetic distance matrix from the SGB
982 phylogeny, scaled to values between 0 and 1 by dividing by its largeste distance. Accordingly,

genome size in megabases and gene counts derived from the number of genes in the prodigal output were included as fixed effect continuous traits. Effect sizes and P-values of the individual models were taken from the summary() function in R. P-values were adjusted for multiple testing by Bonferroni correction. Exemplary phylum-level differences in D-xylose utilization and gene counts between SGBs with and without cophylogeny signals were calculated using non-parametric Fisher's exact and Wilcoxon rank sum test, respectively.

Data availability

All metagenomic sequencing data is available via the NCBI BioProject accession IDs PRJNA692042, PRJNA539933, and PRJNA491335. The collection of 7,700 metagenome-assembled genomes has been deposited in the European Nucleotide Archive, Accession: XXXXX.

Code availability

All code to process sequencing files to generate the presented results and manuscript figures is available via https://github.com/mruehlemann/greatapes_mgx_scripts.

References

Aitchison, J., 1982. The Statistical Analysis of Compositional Data. Journal of the Royal Statistical Society: Series B (Methodological) 44, 139–160. https://doi.org/10.1111/j.2517-6161.1982.tb01195.x

Almeida, A., Nayfach, S., Boland, M., Strozzi, F., Beracochea, M., Shi, Z.J., Pollard, K.S., Sakharova, E., Parks, D.H., Hugenholtz, P., Segata, N., Kyrpides, N.C., Finn, R.D., 2021. A unified catalog of 204,938 reference genomes from the human gut microbiome. Nat Biotechnol 39, 105–114. https://doi.org/10.1038/s41587-020-0603-3

Alneberg, J., Bjarnason, B.S., de Bruijn, I., Schirmer, M., Quick, J., Ijaz, U.Z., Lahti, L., Loman, N.J., Andersson, A.F., Quince, C., 2014. Binning metagenomic contigs by coverage and composition. Nat Methods 11, 1144–1146. https://doi.org/10.1038/nmeth.3103

Amato, K.R., Mallott, E.K., McDonald, D., Dominy, N.J., Goldberg, T., Lambert, J.E., Swedell, L., Metcalf, J.L., Gomez, A., Britton, G.A.O., Stumpf, R.M., Leigh, S.R., Knight, R., 2019. Convergence of human and Old World monkey gut microbiomes demonstrates the importance of human ecology over phylogeny. Genome Biology 20, 201. https://doi.org/10.1186/s13059-019-1807-z

Arnold, C., Matthews, L.J., Nunn, C.L., 2010. The 10kTrees website: A new online resource for primate phylogeny. Evolutionary Anthropology: Issues, News, and Reviews 19, 114–118. https://doi.org/10.1002/evan.20251

1020 Arumugam, M., Raes, J., Pelletier, E., Le Paslier, D., Yamada, T., Mende, D.R., Fernandes,
1021 G.R., Tap, J., Bruls, T., Batto, J.-M., Bertalan, M., Borruel, N., Casellas, F., Fernandez,
1022 L., Gautier, L., Hansen, T., Hattori, M., Hayashi, T., Kleerebezem, M., Kurokawa, K.,
1023 Leclerc, M., Levenez, F., Manichanh, C., Nielsen, H.B., Nielsen, T., Pons, N., Poulain,
1024 J., Qin, J., Sicheritz-Ponten, T., Tims, S., Torrents, D., Ugarte, E., Zoetendal, E.G.,
1025 Wang, J., Guarner, F., Pedersen, O., de Vos, W.M., Brunak, S., Doré, J., MetaHIT
1026 Consortium, Antolín, M., Artiguenave, F., Blottiere, H.M., Almeida, M., Brechot, C.,
1027 Cara, C., Chervaux, C., Cultrone, A., Delorme, C., Denariaz, G., Dervyn, R., Foerstner,
1028 K.U., Friss, C., van de Guchte, M., Guedon, E., Haimet, F., Huber, W., van Hylckama-
1029 Vlieg, J., Jamet, A., Juste, C., Kaci, G., Knol, J., Lakhdari, O., Layec, S., Le Roux, K.,
1030 Maguin, E., Mérieux, A., Melo Minardi, R., M'rini, C., Muller, J., Oozeer, R., Parkhill, J.,
1031 Renault, P., Rescigno, M., Sanchez, N., Sunagawa, S., Torrejon, A., Turner, K.,
1032 Vandemeulebrouck, G., Varela, E., Winogradsky, Y., Zeller, G., Weissenbach, J.,
1033 Ehrlich, S.D., Bork, P., 2011. Enterotypes of the human gut microbiome. Nature 473,
1034 174–180. https://doi.org/10.1038/nature09944
1035 Bankevich, A., Nurk, S., Antipov, D., Gurevich, A.A., Dvorkin, M., Kulikov, A.S., Lesin, V.M.,
1036 Nikolenko, S.I., Pham, S., Prjibelski, A.D., Pyshkin, A.V., Sirotkin, A.V., Vyahhi, N.,
1037 Tesler, G., Alekseyev, M.A., Pevzner, P.A., 2012. SPAdes: A New Genome Assembly
1038 Algorithm and Its Applications to Single-Cell Sequencing. J Comput Biol 19, 455–477.
1039 https://doi.org/10.1089/cmb.2012.0021
1040 Bansal, M.S., Kellis, M., Kordi, M., Kundu, S., 2018. RANGER-DTL 2.0: rigorous reconstruction
1041 of gene-family evolution by duplication, transfer and loss. Bioinformatics 34, 3214–
1042 3216. https://doi.org/10.1093/bioinformatics/bty314
1043 BBMap [WWW Document], n.d. . SourceForge. URL
1044 https://sourceforge.net/projects/bbmap/ (accessed 12.1.22).
1045 Blekhman, R., Tang, K., Archie, E.A., Barreiro, L.B., Johnson, Z.P., Wilson, M.E., Kohn, J.,
1046 Yuan, M.L., Gesquiere, L., Grieneisen, L.E., Tung, J., 2016. Common methods for fecal
1047 sample storage in field studies yield consistent signatures of individual identity in
1048 microbiome sequencing data. Sci Rep 6, 31519. https://doi.org/10.1038/srep31519
1049 Brooks, A.W., Kohl, K.D., Brucker, R.M., Opstal, E.J. van, Bordenstein, S.R., 2016.
1050 Phylosymbiosis: Relationships and Functional Effects of Microbial Communities
1051 across Host Evolutionary History. PLOS Biology 14, e2000225.
1052 https://doi.org/10.1371/journal.pbio.2000225
1053 Campbell, T.P., Sun, X., Patel, V.H., Sanz, C., Morgan, D., Dantas, G., 2020. The microbiome
1054 and resistome of chimpanzees, gorillas, and humans across host lifestyle and
1055 geography. ISME J 14, 1584–1599. https://doi.org/10.1038/s41396-020-0634-2
1056 Cantalapiedra, C.P., Hernández-Plaza, A., Letunic, I., Bork, P., Huerta-Cepas, J., 2021.
1057 eggNOG-mapper v2: Functional Annotation, Orthology Assignments, and Domain
1058 Prediction at the Metagenomic Scale. Molecular Biology and Evolution 38, 5825–
1059 5829. https://doi.org/10.1093/molbev/msab293
1060 Casiano-Colón, A., Marquis, R.E., 1988. Role of the arginine deiminase system in protecting
1061 oral bacteria and an enzymatic basis for acid tolerance. Appl Environ Microbiol 54,
1062 1318–1324.
1063 Chaumeil, P.-A., Mussig, A.J., Hugenholtz, P., Parks, D.H., 2022. GTDB-Tk v2: memory
1064 friendly classification with the genome taxonomy database. Bioinformatics 38, 5315–
1065 5316. https://doi.org/10.1093/bioinformatics/btac672

1066 Costa, F.R.C., Françozo, M.C.S., de Oliveira, G.G., Ignacio, A., Castoldi, A., Zamboni, D.S.,
1067 Ramos, S.G., Câmara, N.O., de Zoete, M.R., Palm, N.W., Flavell, R.A., Silva, J.S., Carlos,
1068 D., 2016. Gut microbiota translocation to the pancreatic lymph nodes triggers NOD2
1069 activation and contributes to T1D onset. J Exp Med 213, 1223–1239.
1070 https://doi.org/10.1084/jem.20150744
1071 Costea, P.I., Hildebrand, F., Arumugam, M., Bäckhed, F., Blaser, M.J., Bushman, F.D., de Vos,
1072 W.M., Ehrlich, S.D., Fraser, C.M., Hattori, M., Huttenhower, C., Jeffery, I.B., Knights,
1073 D., Lewis, J.D., Ley, R.E., Ochman, H., O'Toole, P.W., Quince, C., Relman, D.A.,
1074 Shanahan, F., Sunagawa, S., Wang, J., Weinstock, G.M., Wu, G.D., Zeller, G., Zhao, L.,
1075 Raes, J., Knight, R., Bork, P., 2018. Enterotypes in the landscape of gut microbial
1076 community composition. Nat Microbiol 3, 8–16. https://doi.org/10.1038/s41564-
1077 017-0072-8
1078 Davidson, A.L., Chen, J., 2004. ATP-binding cassette transporters in bacteria. Annu Rev
1079 Biochem 73, 241–268. https://doi.org/10.1146/annurev.biochem.73.011303.073626
1080 Deleu, S., Machiels, K., Raes, J., Verbeke, K., Vermeire, S., 2021. Short chain fatty acids and
1081 its producing organisms: An overlooked therapy for IBD? EBioMedicine 66, 103293.
1082 https://doi.org/10.1016/j.ebiom.2021.103293
1083 Ejby, M., Fredslund, F., Andersen, J.M., Vujičić Žagar, A., Henriksen, J.R., Andersen, T.L.,
1084 Svensson, B., Slotboom, D.J., Abou Hachem, M., 2016. An ATP Binding Cassette
1085 Transporter Mediates the Uptake of α-(1,6)-Linked Dietary Oligosaccharides in
1086 Bifidobacterium and Correlates with Competitive Growth on These Substrates. J Biol
1087 Chem 291, 20220–20231. https://doi.org/10.1074/jbc.M116.746529
1088 Faith, D.P., 1992. Conservation evaluation and phylogenetic diversity. Biological
1089 Conservation 61, 1–10. https://doi.org/10.1016/0006-3207(92)91201-3
1090 Ghazisaeedi, F., Meens, J., Hansche, B., Maurischat, S., Schwerk, P., Goethe, R., Wieler, L.H.,
1091 Fulde, M., Tedin, K., 2022. A virulence factor as a therapeutic: the probiotic
1092 Enterococcus faecium SF68 arginine deiminase inhibits innate immune signaling
1093 pathways. Gut Microbes 14, 2106105.
1094 https://doi.org/10.1080/19490976.2022.2106105
1095 Giuffrè, A., Borisov, V.B., Arese, M., Sarti, P., Forte, E., 2014. Cytochrome bd oxidase and
1096 bacterial tolerance to oxidative and nitrosative stress. Biochimica et Biophysica Acta
1097 (BBA) - Bioenergetics, 18th European Bioenergetics Conference 2014 Lisbon,
1098 Portugal 1837, 1178–1187. https://doi.org/10.1016/j.bbabio.2014.01.016
1099 Gloor, G.B., Macklaim, J.M., Pawlowsky-Glahn, V., Egozcue, J.J., 2017. Microbiome Datasets
1100 Are Compositional: And This Is Not Optional. Frontiers in Microbiology 8.
1101 Gogarten, J.F., Rühlemann, M., Archie, E., Tung, J., Akoua-Koffi, C., Bang, C., Deschner, T.,
1102 Muyembe-Tamfun, J.-J., Robbins, M.M., Schubert, G., Surbeck, M., Wittig, R.M.,
1103 Zuberbühler, K., Baines, J.F., Franke, A., Leendertz, F.H., Calvignac-Spencer, S., 2021.
1104 Primate phageomes are structured by superhost phylogeny and environment.
1105 Proceedings of the National Academy of Sciences 118, e2013535118.
1106 https://doi.org/10.1073/pnas.2013535118
1107 Gorvitovskaia, A., Holmes, S.P., Huse, S.M., 2016. Interpreting Prevotella and Bacteroides as
1108 biomarkers of diet and lifestyle. Microbiome 4, 15. https://doi.org/10.1186/s40168-
1109 016-0160-7
1110 Groussin, M., Mazel, F., Alm, E.J., 2020. Co-evolution and Co-speciation of Host-Gut Bacteria
1111 Systems. Cell Host & Microbe 28, 12–22.
1112 https://doi.org/10.1016/j.chom.2020.06.013

1113 Groussin, M., Mazel, F., Sanders, J.G., Smillie, C.S., Lavergne, S., Thuiller, W., Alm, E.J., 2017.
1114 Unraveling the processes shaping mammalian gut microbiomes over evolutionary
1115 time. Nat Commun 8, 14319. https://doi.org/10.1038/ncomms14319
1116 Groussin, M., Poyet, M., Sistiaga, A., Kearney, S.M., Moniz, K., Noel, M., Hooker, J., Gibbons,
1117 S.M., Segurel, L., Froment, A., Mohamed, R.S., Fezeu, A., Juimo, V.A., Lafosse, S.,
1118 Tabe, F.E., Girard, C., Iqaluk, D., Nguyen, L.T.T., Shapiro, B.J., Lehtimäki, J.,
1119 Ruokolainen, L., Kettunen, P.P., Vatanen, T., Sigwazi, S., Mabulla, A., Domínguez-
1120 Rodrigo, M., Nartey, Y.A., Agyei-Nkansah, A., Duah, A., Awuku, Y.A., Valles, K.A.,
1121 Asibey, S.O., Afihene, M.Y., Roberts, L.R., Plymoth, A., Onyekwere, C.A., Summons,
1122 R.E., Xavier, R.J., Alm, E.J., 2021. Elevated rates of horizontal gene transfer in the
1123 industrialized human microbiome. Cell 184, 2053-2067.e18.
1124 https://doi.org/10.1016/j.cell.2021.02.052
1125 Guindon, S., Dufayard, J.-F., Lefort, V., Anisimova, M., Hordijk, W., Gascuel, O., 2010. New
1126 Algorithms and Methods to Estimate Maximum-Likelihood Phylogenies: Assessing
1127 the Performance of PhyML 3.0. Systematic Biology 59, 307–321.
1128 https://doi.org/10.1093/sysbio/syq010
1129 Hansen, L.B.S., Roager, H.M., Søndertoft, N.B., Gøbel, R.J., Kristensen, M., Vallès-Colomer,
1130 M., Vieira-Silva, S., Ibrügger, S., Lind, M.V., Mærkedahl, R.B., Bahl, M.I., Madsen,
1131 M.L., Havelund, J., Falony, G., Tetens, I., Nielsen, T., Allin, K.H., Frandsen, H.L.,
1132 Hartmann, B., Holst, J.J., Sparholt, M.H., Holck, J., Blennow, A., Moll, J.M., Meyer,
1133 A.S., Hoppe, C., Poulsen, J.H., Carvalho, V., Sagnelli, D., Dalgaard, M.D., Christensen,
1134 A.F., Lydolph, M.C., Ross, A.B., Villas-Bôas, S., Brix, S., Sicheritz-Pontén, T., Buschard,
1135 K., Linneberg, A., Rumessen, J.J., Ekstrøm, C.T., Ritz, C., Kristiansen, K., Nielsen, H.B.,
1136 Vestergaard, H., Færgeman, N.J., Raes, J., Frøkiær, H., Hansen, T., Lauritzen, L.,
1137 Gupta, R., Licht, T.R., Pedersen, O., 2018. A low-gluten diet induces changes in the
1138 intestinal microbiome of healthy Danish adults. Nat Commun 9, 4630.
1139 https://doi.org/10.1038/s41467-018-07019-x
1140 Hauser, M., Steinegger, M., Söding, J., 2016. MMseqs software suite for fast and deep
1141 clustering and searching of large protein sequence sets. Bioinformatics 32, 1323–
1142 1330. https://doi.org/10.1093/bioinformatics/btw006
1143 Hildebrand, F., Gossmann, T.I., Frioux, C., Özkurt, E., Myers, P.N., Ferretti, P., Kuhn, M.,
1144 Bahram, M., Nielsen, H.B., Bork, P., 2021. Dispersal strategies shape persistence and
1145 evolution of human gut bacteria. Cell Host & Microbe 29, 1167-1176.e9.
1146 https://doi.org/10.1016/j.chom.2021.05.008
1147 Hommola, K., Smith, J.E., Qiu, Y., Gilks, W.R., 2009. A permutation test of host-parasite
1148 cospeciation. Mol Biol Evol 26, 1457–1468. https://doi.org/10.1093/molbev/msp062
1149 Huerta-Cepas, J., Szklarczyk, D., Heller, D., Hernández-Plaza, A., Forslund, S.K., Cook, H.,
1150 Mende, D.R., Letunic, I., Rattei, T., Jensen, L.J., von Mering, C., Bork, P., 2019.
1151 eggNOG 5.0: a hierarchical, functionally and phylogenetically annotated orthology
1152 resource based on 5090 organisms and 2502 viruses. Nucleic Acids Res 47, D309–
1153 D314. https://doi.org/10.1093/nar/gky1085
1154 Hyatt, D., Chen, G.-L., LoCascio, P.F., Land, M.L., Larimer, F.W., Hauser, L.J., 2010. Prodigal:
1155 prokaryotic gene recognition and translation initiation site identification. BMC
1156 Bioinformatics 11, 119. https://doi.org/10.1186/1471-2105-11-119
1157 Iljazovic, A., Amend, L., Galvez, E.J.C., de Oliveira, R., Strowig, T., 2021. Modulation of
1158 inflammatory responses by gastrointestinal Prevotella spp. – From associations to

1159 functional studies. International Journal of Medical Microbiology 311, 151472.
1160 https://doi.org/10.1016/j.ijmm.2021.151472
1161 Introducing RemoveHuman: Human Contaminant Removal [WWW Document], 2014. .
1162 SEQanswers. URL
1163 https://www.seqanswers.com/forum/bioinformatics/bioinformatics-aa/37175-
1164 introducing-removehuman-human-contaminant-removal (accessed 8.11.23).
1165 Jaccard, P., 1912. The Distribution of the Flora in the Alpine Zone.1. New Phytologist 11, 37–
1166 50. https://doi.org/10.1111/j.1469-8137.1912.tb05611.x
1167 Jain, C., Rodriguez-R, L.M., Phillippy, A.M., Konstantinidis, K.T., Aluru, S., 2018. High
1168 throughput ANI analysis of 90K prokaryotic genomes reveals clear species
1169 boundaries. Nat Commun 9, 5114. https://doi.org/10.1038/s41467-018-07641-9
1170 Jha, A.R., Davenport, E.R., Gautam, Y., Bhandari, D., Tandukar, S., Ng, K.M., Fragiadakis, G.K.,
1171 Holmes, S., Gautam, G.P., Leach, J., Sherchand, J.B., Bustamante, C.D., Sonnenburg,
1172 J.L., 2018. Gut microbiome transition across a lifestyle gradient in Himalaya. PLoS
1173 Biol 16, e2005396. https://doi.org/10.1371/journal.pbio.2005396
1174 Johnson, A.J., Vangay, P., Al-Ghalith, G.A., Hillmann, B.M., Ward, T.L., Shields-Cutler, R.R.,
1175 Kim, A.D., Shmagel, A.K., Syed, A.N., Walter, J., Menon, R., Koecher, K., Knights, D.,
1176 2019. Daily Sampling Reveals Personalized Diet-Microbiome Associations in Humans.
1177 Cell Host & Microbe 25, 789-802.e5. https://doi.org/10.1016/j.chom.2019.05.005
1178 Joossens, M., Huys, G., Cnockaert, M., Preter, V.D., Verbeke, K., Rutgeerts, P., Vandamme,
1179 P., Vermeire, S., 2011. Dysbiosis of the faecal microbiota in patients with Crohn's
1180 disease and their unaffected relatives. Gut 60, 631–637.
1181 https://doi.org/10.1136/gut.2010.223263
1182 Jurtshuk, P., 1996. Bacterial Metabolism, in: Baron, S. (Ed.), Medical Microbiology.
1183 University of Texas Medical Branch at Galveston, Galveston (TX).
1184 Kanehisa, M., Goto, S., 2000. KEGG: kyoto encyclopedia of genes and genomes. Nucleic
1185 Acids Res 28, 27–30. https://doi.org/10.1093/nar/28.1.27
1186 Kang, D.D., Li, F., Kirton, E., Thomas, A., Egan, R., An, H., Wang, Z., 2019. MetaBAT 2: an
1187 adaptive binning algorithm for robust and efficient genome reconstruction from
1188 metagenome assemblies. PeerJ 7, e7359. https://doi.org/10.7717/peerj.7359
1189 Kembel, S.W., Cowan, P.D., Helmus, M.R., Cornwell, W.K., Morlon, H., Ackerly, D.D.,
1190 Blomberg, S.P., Webb, C.O., 2010. Picante: R tools for integrating phylogenies and
1191 ecology. Bioinformatics 26, 1463–1464.
1192 https://doi.org/10.1093/bioinformatics/btq166
1193 Kovatcheva-Datchary, P., Nilsson, A., Akrami, R., Lee, Y.S., De Vadder, F., Arora, T., Hallen, A.,
1194 Martens, E., Björck, I., Bäckhed, F., 2015. Dietary Fiber-Induced Improvement in
1195 Glucose Metabolism Is Associated with Increased Abundance of Prevotella. Cell
1196 Metab 22, 971–982. https://doi.org/10.1016/j.cmet.2015.10.001
1197 Kundu, S., Bansal, M.S., 2018. On the impact of uncertain gene tree rooting on duplication-
1198 transfer-loss reconciliation. BMC Bioinformatics 19, 290.
1199 https://doi.org/10.1186/s12859-018-2269-0
1200 Langergraber, K.E., Prüfer, K., Rowney, C., Boesch, C., Crockford, C., Fawcett, K., Inoue, E.,
1201 Inoue-Muruyama, M., Mitani, J.C., Muller, M.N., Robbins, M.M., Schubert, G.,
1202 Stoinski, T.S., Viola, B., Watts, D., Wittig, R.M., Wrangham, R.W., Zuberbühler, K.,
1203 Pääbo, S., Vigilant, L., 2012. Generation times in wild chimpanzees and gorillas
1204 suggest earlier divergence times in great ape and human evolution. Proc Natl Acad
1205 Sci U S A 109, 15716–15721. https://doi.org/10.1073/pnas.1211740109

1206 Lawrence, J.G., Retchless, A.C., 2009. The Interplay of Homologous Recombination and
1207 Horizontal Gene Transfer in Bacterial Speciation, in: Gogarten, M.B., Gogarten, J.P.,
1208 Olendzenski, L.C. (Eds.), Horizontal Gene Transfer: Genomes in Flux, Methods in
1209 Molecular Biology. Humana Press, Totowa, NJ, pp. 29–53.
1210 https://doi.org/10.1007/978-1-60327-853-9_3
1211 Lee, J., Yang, J., Zhitnitsky, D., Lewinson, O., Rees, D., 2014. Structural and functional
1212 characterization of a heavy metal detoxifying ABC transporter (997.2). The FASEB
1213 Journal 28, 997.2. https://doi.org/10.1096/fasebj.28.1_supplement.997.2
1214 Li, H., 2018. Minimap2: pairwise alignment for nucleotide sequences. Bioinformatics 34,
1215 3094–3100. https://doi.org/10.1093/bioinformatics/bty191
1216 Li, H., Handsaker, B., Wysoker, A., Fennell, T., Ruan, J., Homer, N., Marth, G., Abecasis, G.,
1217 Durbin, R., 1000 Genome Project Data Processing Subgroup, 2009. The Sequence
1218 Alignment/Map format and SAMtools. Bioinformatics 25, 2078–2079.
1219 https://doi.org/10.1093/bioinformatics/btp352
1220 Lloyd-Price, J., Arze, C., Ananthakrishnan, A.N., Schirmer, M., Avila-Pacheco, J., Poon, T.W.,
1221 Andrews, E., Ajami, N.J., Bonham, K.S., Brislawn, C.J., Casero, D., Courtney, H.,
1222 Gonzalez, A., Graeber, T.G., Hall, A.B., Lake, K., Landers, C.J., Mallick, H., Plichta, D.R.,
1223 Prasad, M., Rahnavard, G., Sauk, J., Shungin, D., Vázquez-Baeza, Y., White, R.A.,
1224 Braun, J., Denson, L.A., Jansson, J.K., Knight, R., Kugathasan, S., McGovern, D.P.B.,
1225 Petrosino, J.F., Stappenbeck, T.S., Winter, H.S., Clish, C.B., Franzosa, E.A., Vlamakis,
1226 H., Xavier, R.J., Huttenhower, C., 2019. Multi-omics of the gut microbial ecosystem in
1227 inflammatory bowel diseases. Nature 569, 655–662.
1228 https://doi.org/10.1038/s41586-019-1237-9
1229 Lozupone, C., Lladser, M.E., Knights, D., Stombaugh, J., Knight, R., 2011. UniFrac: an effective
1230 distance metric for microbial community comparison. ISME J 5, 169–172.
1231 https://doi.org/10.1038/ismej.2010.133
1232 Manara, S., Asnicar, F., Beghini, F., Bazzani, D., Cumbo, F., Zolfo, M., Nigro, E., Karcher, N.,
1233 Manghi, P., Metzger, M.I., Pasolli, E., Segata, N., 2019. Microbial genomes from non-
1234 human primate gut metagenomes expand the primate-associated bacterial tree of
1235 life with over 1000 novel species. Genome Biology 20, 299.
1236 https://doi.org/10.1186/s13059-019-1923-9
1237 Marin, J., Battistuzzi, F.U., Brown, A.C., Hedges, S.B., 2017. The Timetree of Prokaryotes:
1238 New Insights into Their Evolution and Speciation. Molecular Biology and Evolution
1239 34, 437–446. https://doi.org/10.1093/molbev/msw245
1240 Matute, J.D., Duan, J., Flak, M.B., Griebel, P., Tascon-Arcila, J.A., Doms, S., Hanley, T.,
1241 Antanaviciute, A., Gundrum, J., Mark Welch, J.L., Sit, B., Abtahi, S., Fuhler, G.M.,
1242 Grootjans, J., Tran, F., Stengel, S.T., White, J.R., Krupka, N., Haller, D., Clare, S.,
1243 Lawley, T.D., Kaser, A., Simmons, A., Glickman, J.N., Bry, L., Rosenstiel, P., Borisy, G.,
1244 Waldor, M.K., Baines, J.F., Turner, J.R., Blumberg, R.S., 2023. Intelectin-1 binds and
1245 alters the localization of the mucus barrier-modifying bacterium Akkermansia
1246 muciniphila. J Exp Med 220, e20211938. https://doi.org/10.1084/jem.20211938
1247 McCall, L.-I., Callewaert, C., Zhu, Q., Song, S.J., Bouslimani, A., Minich, J.J., Ernst, M., Ruiz-
1248 Calderon, J.F., Cavallin, H., Pereira, H.S., Novoselac, A., Hernandez, J., Rios, R.,
1249 Branch, O.H., Blaser, M.J., Paulino, L.C., Dorrestein, P.C., Knight, R., Dominguez-Bello,
1250 M.G., 2020. Home chemical and microbial transitions across urbanization. Nature
1251 microbiology 5, 108. https://doi.org/10.1038/s41564-019-0593-4

McDonald, B.R., Currie, C.R., 2017. Lateral Gene Transfer Dynamics in the Ancient Bacterial Genus Streptomyces. mBio 8, e00644-17. https://doi.org/10.1128/mBio.00644-17

McMurdie, P.J., Holmes, S., 2013. phyloseq: An R Package for Reproducible Interactive Analysis and Graphics of Microbiome Census Data. PLOS ONE 8, e61217. https://doi.org/10.1371/journal.pone.0061217

Minh, B.Q., Nguyen, M.A.T., von Haeseler, A., 2013. Ultrafast Approximation for Phylogenetic Bootstrap. Molecular Biology and Evolution 30, 1188–1195. https://doi.org/10.1093/molbev/mst024

Minh, B.Q., Schmidt, H.A., Chernomor, O., Schrempf, D., Woodhams, M.D., von Haeseler, A., Lanfear, R., 2020. IQ-TREE 2: New Models and Efficient Methods for Phylogenetic Inference in the Genomic Era. Molecular Biology and Evolution 37, 1530–1534. https://doi.org/10.1093/molbev/msaa015

Moeller, A.H., Caro-Quintero, A., Mjungu, D., Georgiev, A.V., Lonsdorf, E.V., Muller, M.N., Pusey, A.E., Peeters, M., Hahn, B.H., Ochman, H., 2016. Cospeciation of gut microbiota with hominids. Science 353, 380–382. https://doi.org/10.1126/science.aaf3951

Moeller, A.H., Li, Y., Mpoudi Ngole, E., Ahuka-Mundeke, S., Lonsdorf, E.V., Pusey, A.E., Peeters, M., Hahn, B.H., Ochman, H., 2014. Rapid changes in the gut microbiome during human evolution. Proceedings of the National Academy of Sciences 111, 16431–16435. https://doi.org/10.1073/pnas.1419136111

Molinaro, A., Bel Lassen, P., Henricsson, M., Wu, H., Adriouch, S., Belda, E., Chakaroun, R., Nielsen, T., Bergh, P.-O., Rouault, C., André, S., Marquet, F., Andreelli, F., Salem, J.-E., Assmann, K., Bastard, J.-P., Forslund, S., Le Chatelier, E., Falony, G., Pons, N., Prifti, E., Quinquis, B., Roume, H., Vieira-Silva, S., Hansen, T.H., Pedersen, H.K., Lewinter, C., Sønderskov, N.B., Køber, L., Vestergaard, H., Hansen, T., Zucker, J.-D., Galan, P., Dumas, M.-E., Raes, J., Oppert, J.-M., Letunic, I., Nielsen, J., Bork, P., Ehrlich, S.D., Stumvoll, M., Pedersen, O., Aron-Wisnewsky, J., Clément, K., Bäckhed, F., 2020. Imidazole propionate is increased in diabetes and associated with dietary patterns and altered microbial ecology. Nat Commun 11, 5881. https://doi.org/10.1038/s41467-020-19589-w

Mossoun, A., Calvignac-Spencer, S., Anoh, A.E., Pauly, M.S., Driscoll, D.A., Michel, A.O., Nazaire, L.G., Pfister, S., Sabwe, P., Thiesen, U., Vogler, B.R., Wiersma, L., Muyembe-Tamfum, J.-J., Karhemere, S., Akoua-Koffi, C., Couacy-Hymann, E., Fruth, B., Wittig, R.M., Leendertz, F.H., Schubert, G., 2017. Bushmeat Hunting and Zoonotic Transmission of Simian T-Lymphotropic Virus 1 in Tropical West and Central Africa. Journal of Virology 91, 10.1128/jvi.02479-16. https://doi.org/10.1128/jvi.02479-16

Nayfach, S., Rodriguez-Mueller, B., Garud, N., Pollard, K.S., 2016. An integrated metagenomics pipeline for strain profiling reveals novel patterns of bacterial transmission and biogeography. Genome Res 26, 1612–1625. https://doi.org/10.1101/gr.201863.115

Nishida, A.H., Ochman, H., 2021. Captivity and the co-diversification of great ape microbiomes. Nat Commun 12, 5632. https://doi.org/10.1038/s41467-021-25732-y

Nissen, J.N., Johansen, J., Allesøe, R.L., Sønderby, C.K., Armenteros, J.J.A., Grønbech, C.H., Jensen, L.J., Nielsen, H.B., Petersen, T.N., Winther, O., Rasmussen, S., 2021. Improved metagenome binning and assembly using deep variational autoencoders. Nat Biotechnol 39, 555–560. https://doi.org/10.1038/s41587-020-00777-4

Nüse, B., Holland, T., Rauh, M., Gerlach, R.G., Mattner, J., 2023. L-arginine metabolism as pivotal interface of mutual host–microbe interactions in the gut. Gut Microbes 15, 2222961. https://doi.org/10.1080/19490976.2023.2222961

Ochman, H., Elwyn, S., Moran, N.A., 1999. Calibrating bacterial evolution. Proceedings of the National Academy of Sciences 96, 12638–12643. https://doi.org/10.1073/pnas.96.22.12638

Ochman, H., Worobey, M., Kuo, C.-H., Ndjango, J.-B.N., Peeters, M., Hahn, B.H., Hugenholtz, P., 2010. Evolutionary Relationships of Wild Hominids Recapitulated by Gut Microbial Communities. PLOS Biology 8, e1000546. https://doi.org/10.1371/journal.pbio.1000546

Oksanen, J., Simpson, G.L., Blanchet, F.G., Kindt, R., Legendre, P., Minchin, P.R., O'Hara, R.B., Solymos, P., Stevens, M.H.H., Szoecs, E., Wagner, H., Barbour, M., Bedward, M., Bolker, B., Borcard, D., Carvalho, G., Chirico, M., Caceres, M.D., Durand, S., Evangelista, H.B.A., FitzJohn, R., Friendly, M., Furneaux, B., Hannigan, G., Hill, M.O., Lahti, L., McGlinn, D., Ouellette, M.-H., Cunha, E.R., Smith, T., Stier, A., Braak, C.J.F.T., Weedon, J., 2022. vegan: Community Ecology Package.

Olm, M.R., Brown, C.T., Brooks, B., Banfield, J.F., 2017. dRep: a tool for fast and accurate genomic comparisons that enables improved genome recovery from metagenomes through de-replication. ISME J 11, 2864–2868. https://doi.org/10.1038/ismej.2017.126

Parks, D.H., Chuvochina, M., Rinke, C., Mussig, A.J., Chaumeil, P.-A., Hugenholtz, P., 2022. GTDB: an ongoing census of bacterial and archaeal diversity through a phylogenetically consistent, rank normalized and complete genome-based taxonomy. Nucleic Acids Res 50, D785–D794. https://doi.org/10.1093/nar/gkab776

Pasolli, E., Asnicar, F., Manara, S., Zolfo, M., Karcher, N., Armanini, F., Beghini, F., Manghi, P., Tett, A., Ghensi, P., Collado, M.C., Rice, B.L., DuLong, C., Morgan, X.C., Golden, C.D., Quince, C., Huttenhower, C., Segata, N., 2019. Extensive Unexplored Human Microbiome Diversity Revealed by Over 150,000 Genomes from Metagenomes Spanning Age, Geography, and Lifestyle. Cell 176, 649-662.e20. https://doi.org/10.1016/j.cell.2019.01.001

Patro, R., Duggal, G., Love, M.I., Irizarry, R.A., Kingsford, C., 2017. Salmon: fast and bias-aware quantification of transcript expression using dual-phase inference. Nat Methods 14, 417–419. https://doi.org/10.1038/nmeth.4197

R Core Team, 2022. R: A Language and Environment for Statistical Computing. R Foundation for Statistical Computing, Vienna, Austria.

Ridley, C.P., Lee, H.Y., Khosla, C., 2008. Evolution of polyketide synthases in bacteria. Proceedings of the National Academy of Sciences 105, 4595–4600. https://doi.org/10.1073/pnas.0710107105

Rodríguez-Daza, M.C., Pulido-Mateos, E.C., Lupien-Meilleur, J., Guyonnet, D., Desjardins, Y., Roy, D., 2021. Polyphenol-Mediated Gut Microbiota Modulation: Toward Prebiotics and Further. Frontiers in Nutrition 8.

Rühlemann, M.C., Wacker, E.M., Ellinghaus, D., Franke, A., 2022. MAGScoT - a fast, lightweight, and accurate bin-refinement tool. Bioinformatics btac694. https://doi.org/10.1093/bioinformatics/btac694

Scally, A., Dutheil, J.Y., Hillier, L.W., Jordan, G.E., Goodhead, I., Herrero, J., Hobolth, A., Lappalainen, T., Mailund, T., Marques-Bonet, T., McCarthy, S., Montgomery, S.H., Schwalie, P.C., Tang, Y.A., Ward, M.C., Xue, Y., Yngvadottir, B., Alkan, C., Andersen,

L.N., Ayub, Q., Ball, E.V., Beal, K., Bradley, B.J., Chen, Y., Clee, C.M., Fitzgerald, S., Graves, T.A., Gu, Y., Heath, P., Heger, A., Karakoc, E., Kolb-Kokocinski, A., Laird, G.K., Lunter, G., Meader, S., Mort, M., Mullikin, J.C., Munch, K., O'Connor, T.D., Phillips, A.D., Prado-Martinez, J., Rogers, A.S., Sajjadian, S., Schmidt, D., Shaw, K., Simpson, J.T., Stenson, P.D., Turner, D.J., Vigilant, L., Vilella, A.J., Whitener, W., Zhu, B., Cooper, D.N., de Jong, P., Dermitzakis, E.T., Eichler, E.E., Flicek, P., Goldman, N., Mundy, N.I., Ning, Z., Odom, D.T., Ponting, C.P., Quail, M.A., Ryder, O.A., Searle, S.M., Warren, W.C., Wilson, R.K., Schierup, M.H., Rogers, J., Tyler-Smith, C., Durbin, R., 2012. Insights into hominid evolution from the gorilla genome sequence. Nature 483, 169–175. https://doi.org/10.1038/nature10842

Schaan, A.P., Sarquis, D., Cavalcante, G.C., Magalhães, L., Sacuena, E.R.P., Costa, J., Fonseca, D., Mello, V.J., Guerreiro, J.F., Ribeiro-dos-Santos, Â., 2021. The structure of Brazilian Amazonian gut microbiomes in the process of urbanisation. npj Biofilms Microbiomes 7, 1–12. https://doi.org/10.1038/s41522-021-00237-0

Schliep, K.P., 2011. phangorn: phylogenetic analysis in R. Bioinformatics 27, 592–593. https://doi.org/10.1093/bioinformatics/btq706

Sievers, F., Wilm, A., Dineen, D., Gibson, T.J., Karplus, K., Li, W., Lopez, R., McWilliam, H., Remmert, M., Söding, J., Thompson, J.D., Higgins, D.G., 2011. Fast, scalable generation of high-quality protein multiple sequence alignments using Clustal Omega. Mol Syst Biol 7, 539. https://doi.org/10.1038/msb.2011.75

Sonnenburg, E.D., Sonnenburg, J.L., 2019. The ancestral and industrialized gut microbiota and implications for human health. Nat Rev Microbiol 17, 383–390. https://doi.org/10.1038/s41579-019-0191-8

Sonnenburg, J.L., Sonnenburg, E.D., 2019. Vulnerability of the industrialized microbiota. Science 366, eaaw9255. https://doi.org/10.1126/science.aaw9255

Steinegger, M., Söding, J., 2017. MMseqs2 enables sensitive protein sequence searching for the analysis of massive data sets. Nat Biotechnol 35, 1026–1028. https://doi.org/10.1038/nbt.3988

Suzuki, T.A., Fitzstevens, J.L., Schmidt, V.T., Enav, H., Huus, K.E., Mbong Ngwese, M., Grießhammer, A., Pfleiderer, A., Adegbite, B.R., Zinsou, J.F., Esen, M., Velavan, T.P., Adegnika, A.A., Song, L.H., Spector, T.D., Muehlbauer, A.L., Marchi, N., Kang, H., Maier, L., Blekhman, R., Ségurel, L., Ko, G., Youngblut, N.D., Kremsner, P., Ley, R.E., 2022. Codiversification of gut microbiota with humans. Science 377, 1328–1332. https://doi.org/10.1126/science.abm7759

Tange, O., 2011. GNU Parallel - The Command-Line Power Tool. ;login: The USENIX Magazine 36, 42–47.

Thingholm, L.B., Bang, C., Rühlemann, M.C., Starke, A., Sicks, F., Kaspari, V., Jandowsky, A., Frölich, K., Ismer, G., Bernhard, A., Bombis, C., Struve, B., Rausch, P., Franke, A., 2021. Ecology impacts the decrease of Spirochaetes and Prevotella in the fecal gut microbiota of urban humans. BMC microbiology 21. https://doi.org/10.1186/s12866-021-02337-5

Tian, J., Utter, D.R., Cen, L., Dong, P.-T., Shi, W., Bor, B., Qin, M., McLean, J.S., He, X., 2022. Acquisition of the arginine deiminase system benefits epiparasitic Saccharibacteria and their host bacteria in a mammalian niche environment. Proc Natl Acad Sci U S A 119, e2114909119. https://doi.org/10.1073/pnas.2114909119

Tiwari, S.K., van der Putten, B.C.L., Fuchs, T.M., Vinh, T.N., Bootsma, M., Oldenkamp, R., La Ragione, R., Matamoros, S., Hoa, N.T., Berens, C., Leng, J., Álvarez, J., Ferrandis-Vila,

M., Ritchie, J.M., Fruth, A., Schwarz, S., Domínguez, L., Ugarte-Ruiz, M., Bethe, A., Huber, C., Johanns, V., Stamm, I., Wieler, L.H., Ewers, C., Fivian-Hughes, A., Schmidt, H., Menge, C., Semmler, T., Schultsz, C., 2023. Genome-wide association reveals host-specific genomic traits in Escherichia coli. BMC Biology 21, 76. https://doi.org/10.1186/s12915-023-01562-w

Toft, C., Andersson, S.G.E., 2010. Evolutionary microbial genomics: insights into bacterial host adaptation. Nat Rev Genet 11, 465–475. https://doi.org/10.1038/nrg2798

Tsujikawa, Y., Ishikawa, S., Sakane, I., Yoshida, K., Osawa, R., 2021. Identification of genes encoding a novel ABC transporter in Lactobacillus delbrueckii for inulin polymers uptake. Sci Rep 11, 16007. https://doi.org/10.1038/s41598-021-95356-1

UNDP (United Nations Development Programme), 2022. Human Development Report 2021-22. UNDP (United Nations Development Programme).

Valles-Colomer, M., Blanco-Míguez, A., Manghi, P., Asnicar, F., Dubois, L., Golzato, D., Armanini, F., Cumbo, F., Huang, K.D., Manara, S., Masetti, G., Pinto, F., Piperni, E., Punčochář, M., Ricci, L., Zolfo, M., Farrant, O., Goncalves, A., Selma-Royo, M., Binetti, A.G., Becerra, J.E., Han, B., Lusingu, J., Amuasi, J., Amoroso, L., Visconti, A., Steves, C.M., Falchi, M., Filosi, M., Tett, A., Last, A., Xu, Q., Qin, N., Qin, H., May, J., Eibach, D., Corrias, M.V., Ponzoni, M., Pasolli, E., Spector, T.D., Domenici, E., Collado, M.C., Segata, N., 2023. The person-to-person transmission landscape of the gut and oral microbiomes. Nature 614, 125–135. https://doi.org/10.1038/s41586-022-05620-1

Valles-Colomer, M., Falony, G., Darzi, Y., Tigchelaar, E.F., Wang, J., Tito, R.Y., Schiweck, C., Kurilshikov, A., Joossens, M., Wijmenga, C., Claes, S., Van Oudenhove, L., Zhernakova, A., Vieira-Silva, S., Raes, J., 2019. The neuroactive potential of the human gut microbiota in quality of life and depression. Nat Microbiol 4, 623–632. https://doi.org/10.1038/s41564-018-0337-x

Vals-Delgado, C., Alcala-Diaz, J.F., Molina-Abril, H., Roncero-Ramos, I., Caspers, M.P.M., Schuren, F.H.J., Van den Broek, T.J., Luque, R., Perez-Martinez, P., Katsiki, N., Delgado-Lista, J., Ordovas, J.M., van Ommen, B., Camargo, A., Lopez-Miranda, J., 2021. An altered microbiota pattern precedes Type 2 diabetes mellitus development: From the CORDIOPREV study. J Adv Res 35, 99–108. https://doi.org/10.1016/j.jare.2021.05.001

van den Boogaart, K.G., Tolosana-Delgado, R., 2008. “compositions”: A unified R package to analyze compositional data. Computers & Geosciences 34, 320–338. https://doi.org/10.1016/j.cageo.2006.11.017

Vangay, P., Johnson, A.J., Ward, T.L., Al-Ghalith, G.A., Shields-Cutler, R.R., Hillmann, B.M., Lucas, S.K., Beura, L.K., Thompson, E.A., Till, L.M., Batres, R., Paw, B., Pergament, S.L., Saenyakul, P., Xiong, M., Kim, A.D., Kim, G., Masopust, D., Martens, E.C., Angkurawaranon, C., McGready, R., Kashyap, P.C., Culhane-Pera, K.A., Knights, D., 2018. US Immigration Westernizes the Human Gut Microbiome. Cell 175, 962-972.e10. https://doi.org/10.1016/j.cell.2018.10.029

Vieira-Silva, S., Sabino, J., Valles-Colomer, M., Falony, G., Kathagen, G., Caenepeel, C., Cleynen, I., van der Merwe, S., Vermeire, S., Raes, J., 2019. Quantitative microbiome profiling disentangles inflammation- and bile duct obstruction-associated microbiota alterations across PSC/IBD diagnoses. Nat Microbiol 4, 1826–1831. https://doi.org/10.1038/s41564-019-0483-9

1437 Wallenborn, J.T., Vonaesch, P., 2022. Intestinal microbiota research from a global
1438 perspective. Gastroenterology Report 10, goac010.
1439 https://doi.org/10.1093/gastro/goac010
1440 Watanabe, F., Bito, T., 2018. Vitamin B12 sources and microbial interaction. Exp Biol Med
1441 (Maywood) 243, 148–158. https://doi.org/10.1177/1535370217746612
1442 Weimann, A., Mooren, K., Frank, J., Pope, P.B., Bremges, A., McHardy, A.C., 2016. From
1443 Genomes to Phenotypes: Traitar, the Microbial Trait Analyzer. mSystems 1,
1444 10.1128/msystems.00101-16. https://doi.org/10.1128/msystems.00101-16
1445 Wickham, H., Averick, M., Bryan, J., Chang, W., McGowan, L.D., François, R., Grolemund, G.,
1446 Hayes, A., Henry, L., Hester, J., Kuhn, M., Pedersen, T.L., Miller, E., Bache, S.M.,
1447 Müller, K., Ooms, J., Robinson, D., Seidel, D.P., Spinu, V., Takahashi, K., Vaughan, D.,
1448 Wilke, C., Woo, K., Yutani, H., 2019. Welcome to the Tidyverse. Journal of Open
1449 Source Software 4, 1686. https://doi.org/10.21105/joss.01686
1450 Wu, Y.-W., Simmons, B.A., Singer, S.W., 2016. MaxBin 2.0: an automated binning algorithm
1451 to recover genomes from multiple metagenomic datasets. Bioinformatics 32, 605–
1452 607. https://doi.org/10.1093/bioinformatics/btv638
1453 Yen, M.-R., Peabody, C.R., Partovi, S.M., Zhai, Y., Tseng, Y.-H., Saier, M.H., 2002. Protein-
1454 translocating outer membrane porins of Gram-negative bacteria. Biochimica et
1455 Biophysica Acta (BBA) - Biomembranes 1562, 6–31. https://doi.org/10.1016/S0005-
1456 2736(02)00359-0
1457 Yu, G., Smith, D.K., Zhu, H., Guan, Y., Lam, T.T.-Y., 2017. ggtree: an r package for visualization
1458 and annotation of phylogenetic trees with their covariates and other associated
1459 data. Methods in Ecology and Evolution 8, 28–36. https://doi.org/10.1111/2041-
1460 210X.12628
1461 Zheng, L., Kelly, C.J., Colgan, S.P., 2015. Physiologic hypoxia and oxygen homeostasis in the
1462 healthy intestine. A Review in the Theme: Cellular Responses to Hypoxia. Am J
1463 Physiol Cell Physiol 309, C350–C360. https://doi.org/10.1152/ajpcell.00191.2015
1464 Zheng, P., Li, Z., Zhou, Z., 2018. Gut microbiome in type 1 diabetes: A comprehensive review.
1465 Diabetes/Metabolism Research and Reviews 34, e3043.
1466 https://doi.org/10.1002/dmrr.3043
1467 Ziyatdinov, A., Vázquez-Santiago, M., Brunel, H., Martinez-Perez, A., Aschard, H., Soria, J.M.,
1468 2018. lme4qtl: linear mixed models with flexible covariance structure for genetic
1469 studies of related individuals. BMC Bioinformatics 19, 68.
1470 https://doi.org/10.1186/s12859-018-2057-x
1471

1472

1473 **Acknowledgements**

1474 We thank the IKMB Microbiome and NGS laboratories for excellent technical support. We
1475 thank Sébastien Calvignac-Spencer and Grit Schubert for their valuable contributions to the
1476 analysis and the manuscript. This study is an outcome of the Deutsche
1477 Forschungsgemeinschaft (DFG) Collaborative Research Center 1182 “Origin and Function of
1478 Metaorganisms” (https://www.metaorganism-research.com, Project number: 261376515,
1479 Projects A2 and Z2) and received infrastructure support from the DFG Excellence Cluster 2167

"Precision Medicine in Chronic Inflammation" (PMI; Project number: 390884018). JFG was supported by the DFG grant “The ecology and evolution of primate phageomes” (GO 3443/1-1: Project number: 453352748) and the DFG Research Group “Sociality and Health in Primates” (FOR2136; CA 1108/3-1; Project number: 244372499). Research at Kokolopori was supported by the Max Planck Society and Harvard University. Research at Ozouga and Taï National Park was supported by the Max Planck Society. Research at Loango was supported by US Fish and Wildlife Service, Tusk Trust, Berggorilla Regenwald Direkthilfe, and the Max Planck Society. Research at Bwindi was supported by the Max Planck Society. The survey of the Bwindi mountain gorillas was funded by the International Gorilla Conservation Programme coalition members with supplemental funding from the Wildlife Conservation Society. We are extremely grateful to the organizations that facilitated work at these field sites for sample collection: Bwindi - The mountain gorilla survey was conducted by the Uganda Wildlife Authority, l’Institut Congolais pour la Conservation de la Nature, the Rwanda Development Board, the International Gorilla Conservation Programme, the Max Planck Institute for Evolutionary Anthropology, Conservation Through Public Health, the Mountain Gorilla Veterinary Project, the Institute for Tropical Forest Conservation, and The Dian Fossey Gorilla Fund; Kokolopori - Vie Sauvage, the Bonobo Conservation Initiative; Loango - Agence Nationale des Parcs Nationaux, the Centre National de la Recherche Scientifique et Technique of Gabon; Taï National Park - the Centre Suisse de Recherches Scientifiques en Côte d’Ivoire and the staff members of the Taï Chimpanzee Project. We thank Taylor Hermes for support in the writing of the manuscript.

Author contributions

J.F.B., F.H.L., and A.F. designed the research project; C.A.-K., C.B., T.D., J.-J.M.-T., M.M.R., M.S., R.M.W., K.Z., A.F., and F.H.L. built and maintained research infrastructure, performed field research, and provided materials. M.R., C.B., J.F.G, M.G., S.W., M.P., J.F.B., F.H.L., and A.F. analyzed data. M.R., B.M.H., C.B., J.F.G., M.G., M.P., M.U., J.F.B., F.H.L., and A.F. wrote the manuscript. All authors read, edited, and approved the submitted version of the manuscript.

Competing Interests

1512 All authors declare no conflicts of interest.

1513 **Figures**

1514

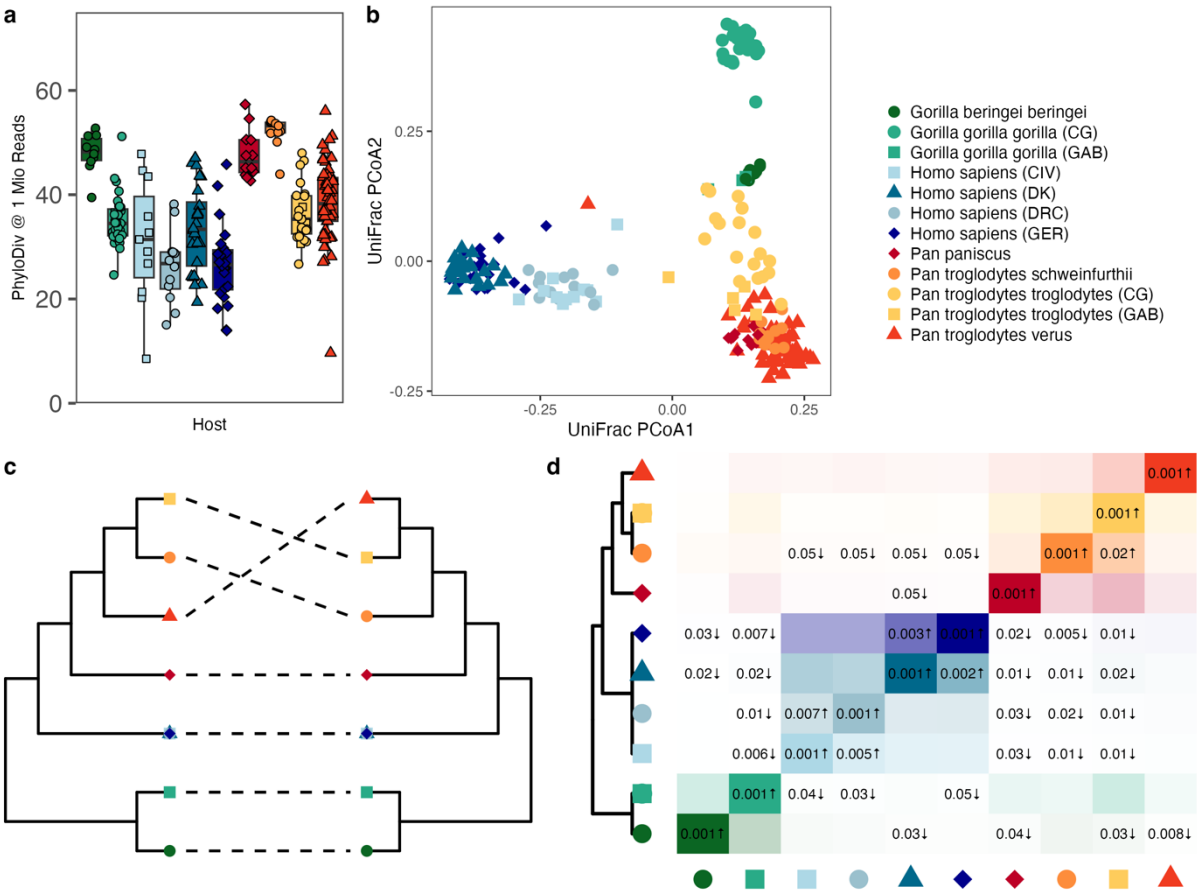

1515

1516 Figure 1: Community-level specificities of human and NHA fecal microbiomes. (a)
1517 Phylogenetic Diversity across host groups at a sampling depth of 1 Mio. mapped reads per
1518 sample. (b) Ordination of unweighted UniFrac distances of all samples, colored by host
1519 subgroups. (c) Tanglegram of host (left) and microbiome (right) trees, the latter based on
1520 unweighted UniFrac distances. (d) SGB sharing coefficients between host group. Rows
1521 represent reference host groups; columns represent the groups with which they share
1522 overlap. Numbers in the tiles are P-values from the analysis for enrichment (#) and
1523 depletion ($) in the reference group. *Boxplots in this and other plots show the following*
1524 *elements: center line: median, box limits: upper and lower quartile; whiskers: 1.5 x*
1525 *interquartile ranges.*

1526

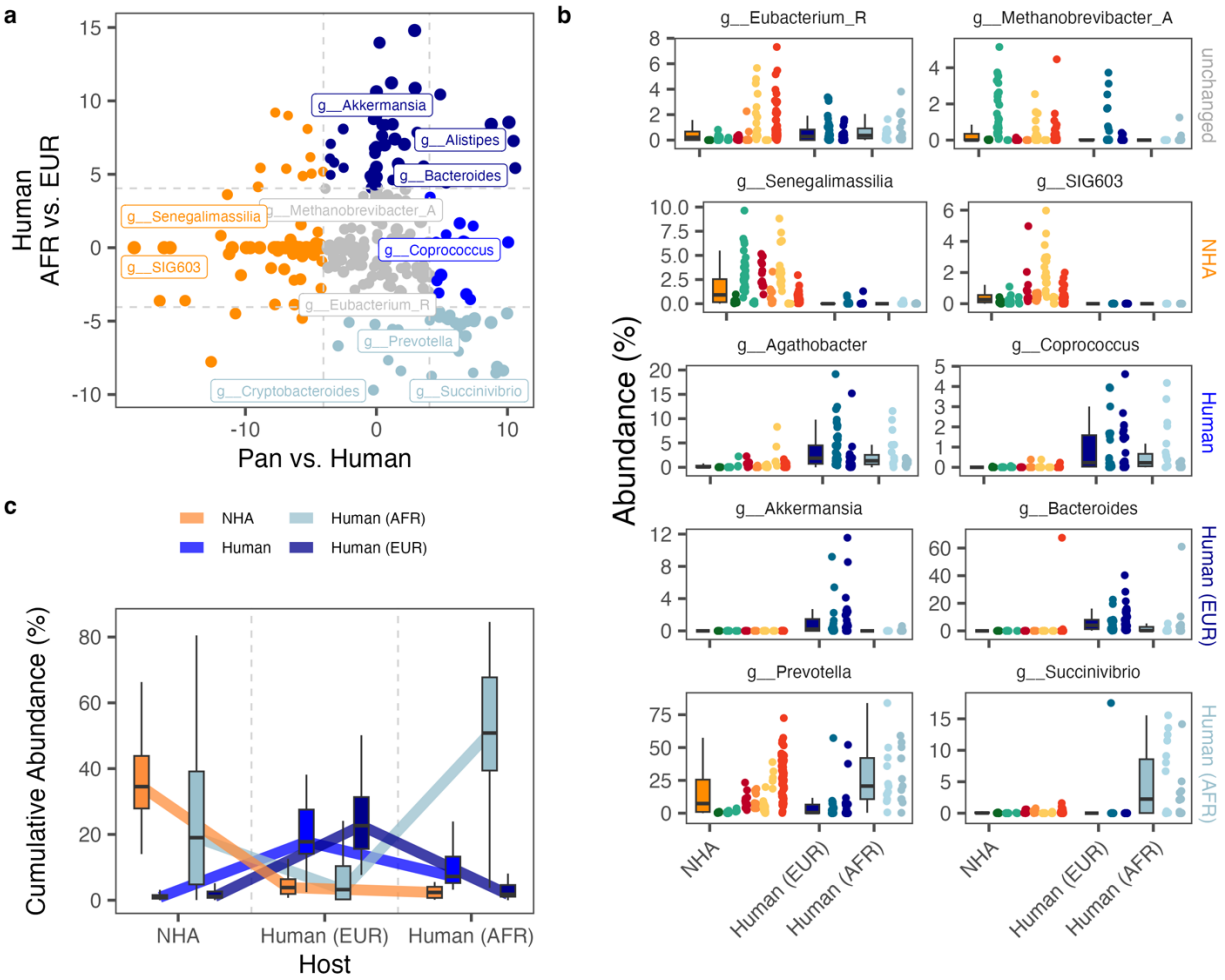

Figure 2: Taxonomic differences the microbiota of humans and NHAs: (a) Effect sizes (t-values from univariate linear regression) of abundance differences of genera in fecal samples of NHAs and humans (x-axis) and humans within African and European populations separated as well (y-axis). Points are colored according to the association groups with European (dark blue) and African human populations (light blue), or to indicate enrichment in NHAs (orange) or humans (bright blue). Taxonomic groups not found to be associated with any of the groups (all Q > 0.05) are shown in grey. Horizontal and vertical lines depict the t-value threshold (|t-value| > 4.04) for statistical significance after Bonferroni-correction. (b) Per-sample and host group abundances of selected genera found with unchanged abundances across all groups (top), increased abundance in NHAs or humans (rows 2 and 3), or in humans from Africa or Europe (rows 4 and 5). Points are colored according to host genus: Gorilla = greens, Pan = reds, oranges, and yellows, and human = blues. (c) Cumulative abundance trajectories of taxa associated with human communities and NHAs. Shown are the per-sample cumulative abundances within each host group, grouped based on a taxon's association with either NHAs, all humans, or one of the human population subgroups.

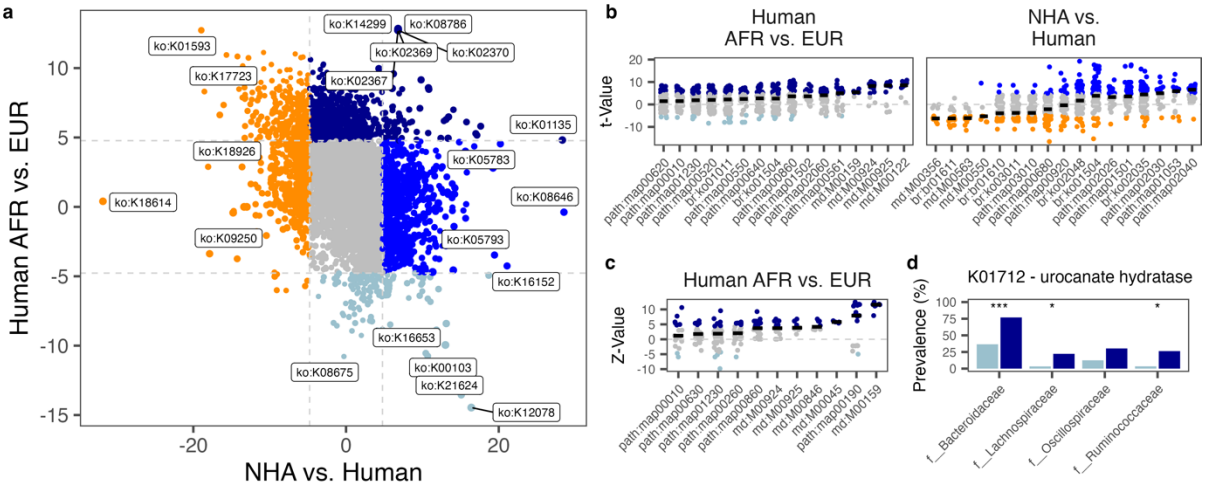

Figure 3: Functional differences in the microbiota of humans and NHAs: (a) Effect sizes (t-values from univariate linear regression) of the abundance differences of KEGG orthologs in fecal samples of NHAs and humans (x-axis) and humans within African and European populations separated as well (y-axis). Points are colored according to the association groups with European (dark blue) and African human populations (light blue), or according to general enrichment in NHAs (orange) or humans (mid-blue). Taxonomic groups not found associated with any of the groups (all Q > 0.05) are shown in grey. Horizontal and vertical lines depict the t-value threshold (|t-value| > 4.77) for statistical significance after Bonferroni-correction. (b) KEGG ortholog (KO) effect sizes for differential abundance between African and European human population associated taxa. Shown KOs are ordered into functional higher-level KEGG categories that were found enriched (QFisher<0.05) among KOs with significantly different abundances between groups. Horizontal bars indicate median t-values of all KOs in a KEGG category as an estimate for the direction of the enrichment. (c) KOs found enriched in the pangenomes of humans from Africa or Europe across four bacterial families shared across continents. Shown are the Z-values of the fixed-effects meta-analysis of KOs for enrichment across microbial families. KOs are sorted into functional higher-level KEGG categories that were found enriched (QFisher<0.05) among KOs with significantly different prevalence (QMeta<0.05) between African and European pangenomes. Horizontal bars depict median ZMeta-values of KOs within higher-level KEGG categories. (d) Prevalence of the urocanate hydratase gene (K01712) in clades found higher abundant in humans from Europe across four microbial families. Stars indicate per-clade differences in gene prevalence: *p < 0.05, **p< 0.01, ***, p<0.001.

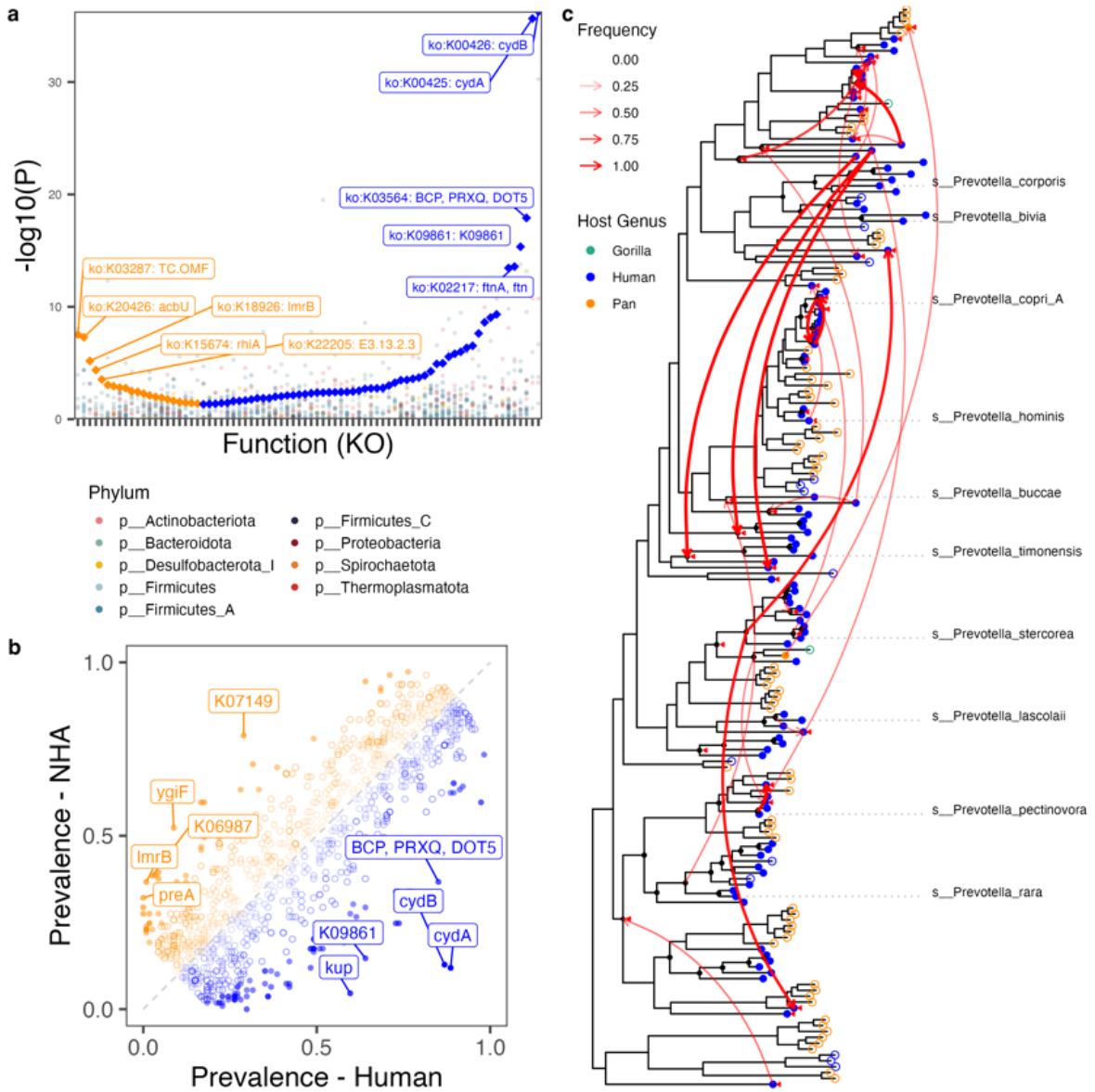

Figure 4: Cross-microbial clade functional associations with NHA and human hosts. (a) KO terms consistently enriched in human- (blue diamonds) and NHA-associated (orange diamonds) taxonomic clades. Individual genus-level P_{Fisher}-values are shown in points colored by phylum. Shown P-values are unadjusted for taxon-level tests and Bonferroni-corrected for multiple testing for the meta-analysis (b) Prevalence patterns of KO terms in human- (blue) and NPH-associated (orange) Prevotella SGBs. Filled shapes represent KOs with significant (Q<0.05) differences in the statistical test. (c) Results of the tree reconciliation analysis for the cydA gene in Prevotella SGBs found in humans (blue) and NHAs (Pan: orange; Gorilla: green) demonstrate a history of frequent transfer events (red arrows) across 1000 reconciliations with random seeds. Filled and empty shapes represent cydA-positive and -negative SGBs, respectively. Arrows are weighted by frequency. Red triangles mark nodes that were identified as gene transfer recipients with > 50% frequency independent of the donor node. Black circles mark speciation events with > 50% frequency. The ten highest abundant Prevotella species with established names are shown for orientation. The Prevotella tree was rooted using Paraprevotella clara as the outgroup (not shown).

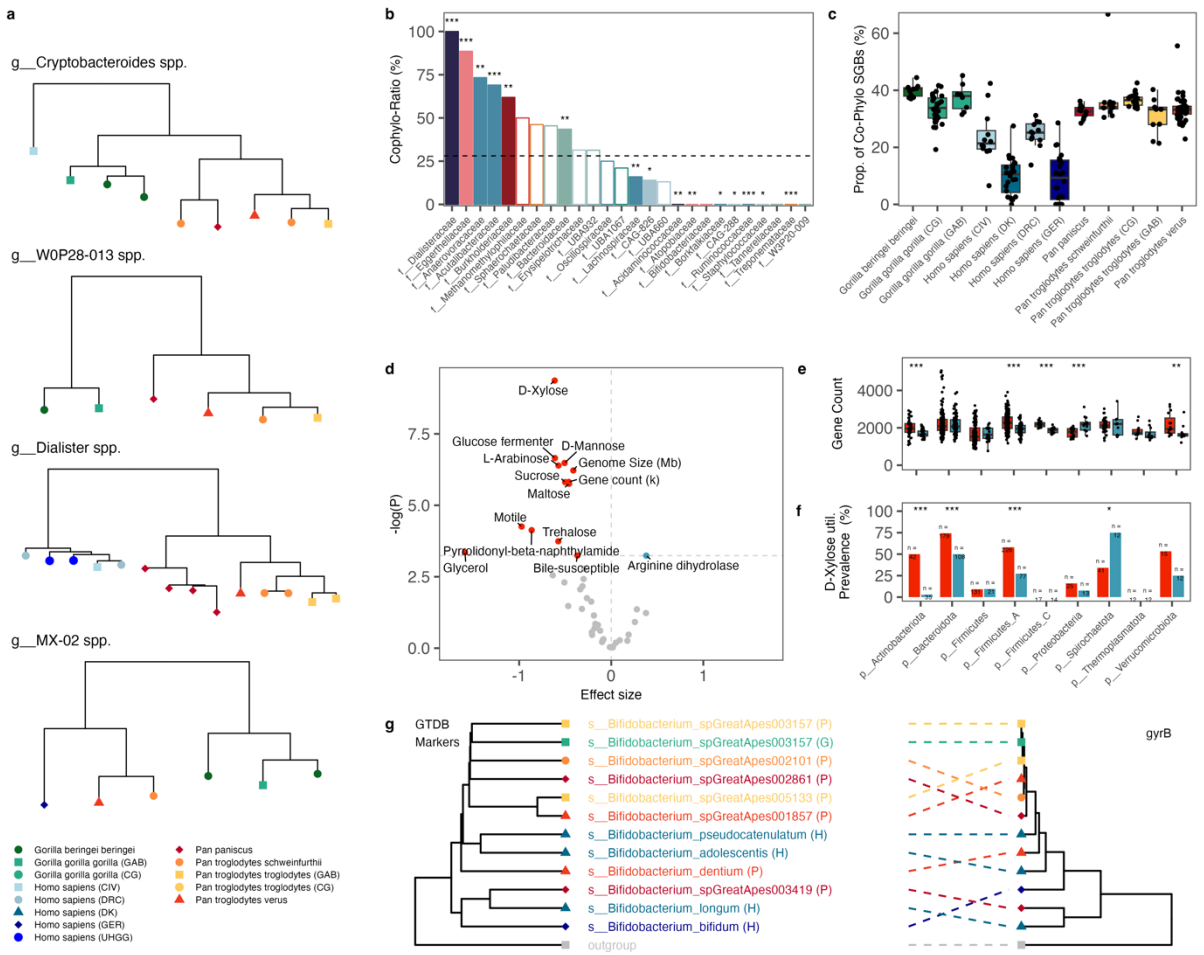

Figure 5: Cophylogeny across humans and non-human African great apes. (a) Subtree phylogenies of groups with significant results in the Mantel-test based analysis for co-phylogeny. Tip colors and shapes correspond to the host subgroups. Trees were rooted on a randomly selected outgroup from a related family (not shown). (b) Enrichment and depletion of co-phylogeny patterns across microbial families with at least 10 SGBs in the analysis. Bars are colored by phylum, corresponding to the colors in Figure 1. Filled bars denote significant (Q<0.05) enrichment and depletion. The dashed line represents the average co-phylogeny ratio across all SGBs. (c) Per-sample proportion of SGBs with co-phylogeny patterns across and colored by host subgroups. (d) Enrichment (blue) and depletion (red) of 43 in-silico inferred microbial traits, genome size and gene count in association with cophylogeny signals. Effect sizes and P-values from mixed effects logistic regression accounting for phylogenetic relatedness of SGBs. The horizontal line marks the threshold of significant Bonferroni-adjusted P-values. (e) SGB-level gene counts across nine phyla, grouped by the presence (blue) and absence (red) of a cophylogeny signal. Within-phylum differences were assessed by two-sided Wilcoxon rank-sum test. (f) Prevalence of inferred D-Xylose utilization by SGBs across phyla, grouped by the presence (blue) and absence (red) of a cophylogeny signal. Within-phylum differences in prevalence were assessed using a two-sided Fisher-test. (g) Tanglegram of Bifidobacterium maximum-likelihood phylogenies based on 120 GTDB marker genes (left) and gyrB sequence (right). Tip colors and shapes correspond to the host subgroups. Across all panels, stars indicate level of significance: * P < 0.05, ** P < 0.01, *** P < 0.001.

1607 **Tables**

1608

1609 Table1: KEGG functional groups with significant enrichment (Q < 0.05) in the gut
1610 microbiome of humans living in Europe.

1611

KEGG ID	Name	# of KOs	Mean Z-Score	P-value	Q-value
md:M00159	V/A-type ATPase, prokaryotes	9	11.19	3.23E-16	2.64E-13
path:map00190	Oxidative phosphorylation	223	5.83	1.39E-08	1.13E-05
md:M00924	Cobalamin biosynthesis, anaerobic, uroporphyrinogen III => sirohydrochlorin => cobyrinate a,c-diamide	22	3.59	2.38E-08	1.94E-05
path:map00860	Porphyrin metabolism	139	3.51	5.08E-08	4.15E-05
md:M00045	Histidine degradation, histidine => N-formiminoglutamate => glutamate	8	5.79	4.37E-07	3.57E-04
path:map00010	Glycolysis / Gluconeogenesis	106	1.81	5.21E-06	4.25E-03
md:M00846	Siroheme biosynthesis, glutamyl-tRNA => siroheme	16	4.64	5.99E-06	4.90E-03
md:M00925	Cobalamin biosynthesis, aerobic, uroporphyrinogen III => precorrin 2 => cobyrinate a,c-diamide	17	4.36	1.07E-05	8.78E-03
path:map00630	Glyoxylate and dicarboxylate metabolism	101	1.94	3.60E-05	2.94E-02
path:map00260	Glycine, serine and threonine metabolism	109	1.74	5.87E-05	4.80E-02
path:map01230	Biosynthesis of amino acids	238	1.41	6.05E-05	4.94E-02

1612

1613